THREE-DIMENSIONAL FINITE ELEMENT ANALYSES FOR OPTIMAL GROUND IMPROVEMENT FOR TUNNEL CROSS PASSAGE IN BANGKOK SUBSOILS

Mr. Mengly Seng

การวิเคราะห์ไฟไนต์อิลิเมนต์แบบสามมิติเพื่อหารูปแบบการปรับปรุงดินที่เหมาะสมสำหรับการสร้างทางเชื่อมอุโมงค์ในชั้นดินกรุงเทพ

นายเมงลี เซง

Thesis Title	THREE-DIMENSIONAL FINITE ELEMENT ANALYSES FOR OPTIMAL GROUND IMPROVEMENT FOR TUNNEL CROSS PASSAGE IN BANGKOK SUBSOILS
By	Mr. Mengly Seng
Field of Study	Civil Engineering
Thesis Advisor	Associate Professor TIRAWAT BOONYATEE, D.Eng.

Accepted by the FACULTY OF ENGINEERING, Chulalongkorn University in Partial Fulfillment of the Requirement for the Master of Engineering

.... Dean of the FACULTY OF ENGINEERING
(Professor SUPOT TEACHAVORASINSKUN, D.Eng.)

THESIS COMMITTEE

.... Chairman
(Veerayut Komolvillas, D.Eng)
.... Thesis Advisor
(Associate Professor TIRAWAT BOONYATEE, D.Eng.)
.... External Examiner
(Associate Professor Pornkasem Jongpradist, Ph.D.)

จุฬาลงกรณ์มหาวิทยาลัย
CHULALONGKORN UNIVERSITY

เมงลี เซง : การวิเคราะห์ไฟไนต์อิลิเมนต์แบบสามมิติเพื่อหารูปแบบการปรับปรุงดินที่เหมาะสมสำหรับการสร้างทางเชื่อมอุโมงค์ในชั้นดินกรุงเทพ. (THREE-DIMENSIONAL FINITE ELEMENT ANALYSES FOR OPTIMAL GROUND IMPROVEMENT FOR TUNNEL CROSS PASSAGE IN BANGKOK SUBSOILS) อ.ที่ปรึกษาหลัก : ฐิรวัตร บุญญะฐี

การฉีดน้ำปูนเป็นวิธีการหนึ่งที่นิยมใช้ในการเพิ่มเสถียรภาพระหว่างการก่อสร้างทางข้ามอุโมงค์ในชั้นดินอ่อน การวิเคราะห์ด้วยวิธีไฟไนต์อิลิเมนต์แบบสามมิติถูกใช้ในการศึกษานี้เพื่อหาขนาดของดินผสมซีเมนต์ที่น้อยที่สุดที่ยังรักษาความปลอดภัยในระหว่างการก่อสร้างไว้ได้ โดยสมมติให้ดินซีเมนต์ถูกปรับปรุงเป็นรูปปริซึมแปดเหลี่ยมที่วิ่งตามแนวการก่อสร้างของทางข้ามอุโมงค์ซึ่งมีรัศมีเท่ากับ 2.25 เมตร ผลการศึกษาแสดงว่าอัตราส่วนปลอดภัยจะเพิ่มขึ้นเป็นเชิงเส้นกับรัศมีของดินผสมซีเมนต์ และเมื่อรัศมีของดินผสมซีเมนต์มีค่าเท่ากับ 3.60 เมตร อัตราส่วนความปลอดภัยจะมีค่าเท่ากับ 1.4 ซึ่งเพียงพอต่อการรักษาเสถียรภาพของป้องกันการไหลซึมของน้ำระหว่างการก่อสร้างได้ นอกจากการวิเคราะห์ด้านเสถียรภาพแล้วยังได้ศึกษาความสัมพันธ์ระหว่างการทรุดตัวที่ผิวดินกับขนาดของการปรับปรุงดินด้วย ซึ่งพบว่าการทรุดตัวที่ผิวดินสามารถอธิบายได้ด้วยสมการที่เสนอโดย Peck และ O'Reilly โดยใช้ค่าคงที่เชิงประสบการณ์ (K) เท่ากับ 0.6 ซึ่งได้จากการเฉลี่ยถ่วงน้ำหนักตามความหนาระหว่างค่าคงที่เชิงประสบการณ์ของชั้นดินเหนียวแข็งและชั้นดินเหนียวอ่อนซึ่งมีค่าเท่ากับ 0.4 และ 0.7 ตามลำดับ

สาขาวิชา	วิศวกรรมโยธา	ลายมือชื่อนิสิต
		....
ปีการศึกษา	2563	ลายมือชื่อ อ.ที่ปรึกษาหลัก
		....

6170505921 : MAJOR CIVIL ENGINEERING
KEYWORD: CROSS PASSAGE, TUNNEL, OPTIMIZATION, FINITE ELEMENT
                    ANALYSIS, BANGKOK CLAY, SOIL-CEMENT MIXING, GROUND
                    IMPROVEMENT
            Mengly Seng : THREE-DIMENSIONAL FINITE ELEMENT ANALYSES FOR
            OPTIMAL GROUND IMPROVEMENT FOR TUNNEL CROSS PASSAGE IN
            BANGKOK SUBSOILS. Advisor: Assoc. Prof. TIRAWAT BOONYATEE,
            D.Eng.

Jet grouting is a common technic for improving the stability during the construction of tunnel cross-passages in soft grounds. In this study, the optimal soil-cement mass for a cross-passage from a tunnel to an intervention shaft in Bangkok subsoils was determined using three-dimensional finite element analyses. The soil-cement mass was assumed to be octagonal prism along the route of the cross-passage which has the radius of 2.25m. The result showed that the factor of safety increases linearly with the improvement radius. The improvement radius of 3.60m was selected since it is satisfied with the FS more than 1.4 and the thickness is more than 0.1m to prevent from the short-term seepage problem. In addition, the relationship between the improved groundmass and ground surface settlement curve was made. It was found that the predicted settlement profile can be captured by the formula proposed by Peck and O'Reilly providing that the empirical coefficient of 0.6 agrees well with the results from the 3D simulation and this value was obtained from the average of K = 0.4 and K = 0.7 which is the empirical coefficient value of stiff clay and soft clay respectively based on the overburden thickness.

จุฬาลงกรณ์มหาวิทยาลัย
CHULALONGKORN UNIVERSITY

Field of Study:	Civil Engineering	Student's Signature ....
Academic Year:	2020	Advisor's Signature ....

ACKNOWLEDGEMENTS

TABLE OF CONTENTS

Page

จุฬาลงกรณ์มหาวิทยาลัย

CHULALONGKORN UNIVERSITY

LIST OF TABLES

LIST OF FIGURES

จุฬาลงกรณ์มหาวิทยาลัย

CHULALONGKORN UNIVERSITY

CHAPTER 1

INTRODUCTION

1.1 Motivation and Problem Statement

Bangkok is the capital city of Thailand, where urban pollution increases significantly. Therefore, the number of constructions is increased by the demand of the city's development and citizens. These constructions also include underground facilities such as underground railway system, sewage system, drainage system which are essential for sustainable developments. For transportation tunnels, they must be stable and safe. Evacuation measures when an accident occurs are generally compulsory for every tunnel. One of common measures is to provide cross-passage from a tunnel to another tunnel or from a tunnel to an intervention shaft (IVS) so that passengers are not trapped inside during an incident. Most of MRT tunnels in Bangkok are connected to IVSs.

Since underground constructions in Bangkok are performed in soft soil layers, a great attention shall be paid for preventing excessive ground deformation and ground's instability. In general, tunnel works in Bangkok's stiff clay induce surface settlements in a range of 25~50 mm Sirivachiraporn and Phienwej (2012). Ground stabilizations are needed in some areas when this magnitude of settlement is not acceptable.

In tunnelling construction, many ground stabilization methods are proposed such as pipe roof method, ground freezing method, forepoling method, grouting method, and deep soil mixing method. These methods are classified as pre-support methods for stabilizing the soil in tunnel construction. The deep soil mixing method is an effective method which has been used widely for excavation support, particularly where there are concerns about settlement, groundwater control, flowing of ground (Tunnel stability) or contamination (Waste protection and groundwater contamination). The deep soil mixing method turns soft ground into soil-cement by mixing Portland cement, water and existing soil. This mixture is considered as week concrete which is

durable and can be employed at a low cost. Nonetheless, the construction cost can be reduced further by optimizing the amount of cement.

There are a number of researches on the applications of deep soil mixing method (DMM) for deep excavations, embankments, and foundations. However, the application of the DMM on tunnel cross-passages in Bangkok is not much. Therefore, the optimum use of cement for this application is performed in this study.

1.2 Research Objectives

The objectives of the thesis are:

- To optimize the extent of ground improvement by deep soil mixing method with the consideration of ground stability and deformation requirements.
- To evaluate the effect of improvement patterns on the performance of tunnel cross-passages.

1.3 Scopes and Limitations

To achieve the above objectives, the study will be performed by a three-dimensional finite element analysis code (PLAXIS 3D). The cross-passages will be modelled by the excavation from an existing tunnel to an intervention shaft which is commonly adopted in Bangkok. Nonetheless, the concept of the design is similar to the cross-passage which connects between two tunnels.

In this study, the Bangkok subsoil is simplified into three layers although the real geological is more complex, i.e., varied layers in different zones. The three subsoil layers are listed as followed:

- 1st layer: Soft to Medium Bangkok clay
- 2nd layer: Stiff clay
- 3rd layer: Dense sand

The cross-passage in the study is excavated from an existing tunnel to an intervention vertical shaft (IVS) in horizontal direction (without changing the elevation). Since most of cross-passage in Bangkok was constructed by the sequential excavation

method, the cross-passage in this study is assumed to a horseshoe shape. Furthermore, the displacement induced by the construction of tunnel and IVS is excluded in this study. Finally, although the construction in this study occurs in soft soils, the consolidation settlement is not considered in this research.

1.4 Research Outcome

The study will be beneficial for

- The optimum use of deep soil mixing method and cement for the construction of tunnel cross-passage.
- The mitigation of ground settlement due to underground construction.
- Further researches on deep soil-cement mixing and civil engineering practices.

CHAPTER 2
LITERATURE REVIEW

2.1 Subsoil Condition in Bangkok

Ground condition in Bangkok is known for a thick layer of soil clay because this city is situated on the delta of Chao Phraya River and the Gulf of Thailand. Additionally, it is a kind of marine soft clay which has deposited since the Quaternary period (Surarak et al., 2012). Furthermore, Bangkok subsoil is non-homogeneous and complicated.
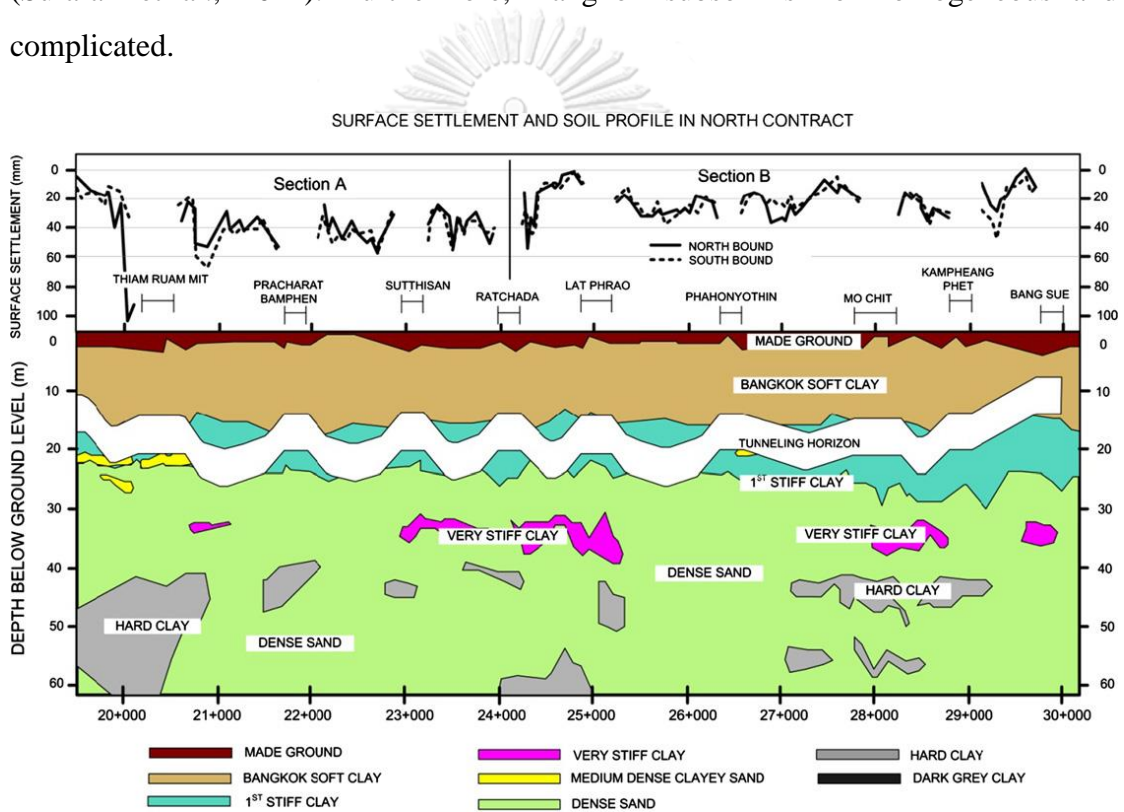
Figure 2-1. Soil profile of the Bangkok MRT blue line North tunnel section
(Sirivachiraporn & Phienwej, 2012)

Figure 2-1 indicated that Bangkok subsoil is complicated because it is not uniform and composed of clayey sand deposit in the stiff clay formation. Soil formation in some areas in Bangkok can have four layers or more.

The model of subsoil in this study is prepared following the section A of the MRT blue line in Bangkok (Figure 2-2).
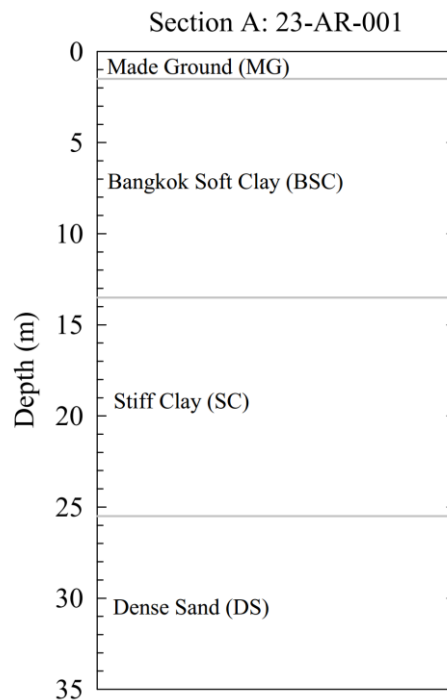
Figure 2-2 Soil profile in section A of the MRT blue line (Likitlersuang et al., 2014)

2.2 Groundwater Condition in Bangkok

In the last decade, Bangkok has undergone groundwater drawdown caused by extensive pumping well. The ground water pressure in Bangkok increases along depth from zero kPa at 1m below ground surface. However, the pressure decreases along depth in the stiff clay layer before increases again at the depth around 22 m as shown in Figure 2-3. It shall be noted that at present the groundwater table has been increasing due to a recent restriction on groundwater pumping. Therefore, the distribution of water pressure in Figure 2-3 may not represent the current condition.
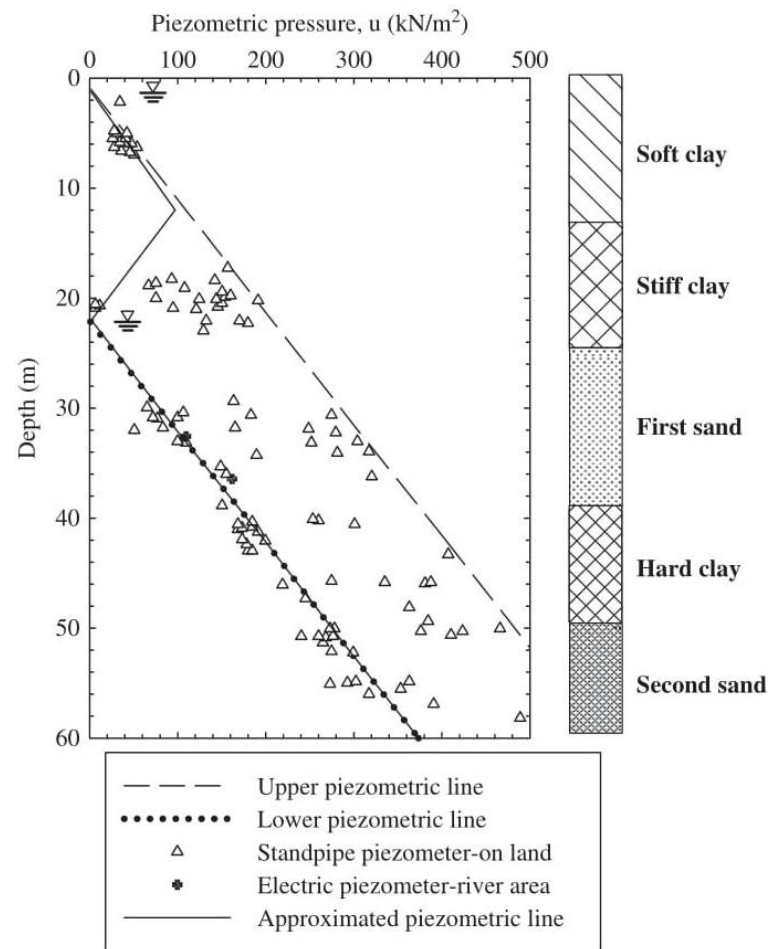
Figure 2-3. Pore water pressure in Bangkok subsoil (Surarak et al., 2012)

Saowiang and Giao (2020) numerically analyzed surface displacements due to groundwater variations in Bangkok at 6 locations (Figure 2-4). The groundwater levels at six boreholes tend to increase linearly during 1997 to 2013 as shown in Figure 2-4. Since the BH1 is near the Lat Phrao station, it is selected for the study in the research. The red-dash line indicates the prediction of the groundwater level in the future (2030) which is assumed to be the full recovery time of groundwater system. The groundwater level at -10m is assumed in the research based on the data from the PD0034 monitoring station where is the nearest to the Lat Phrao station.
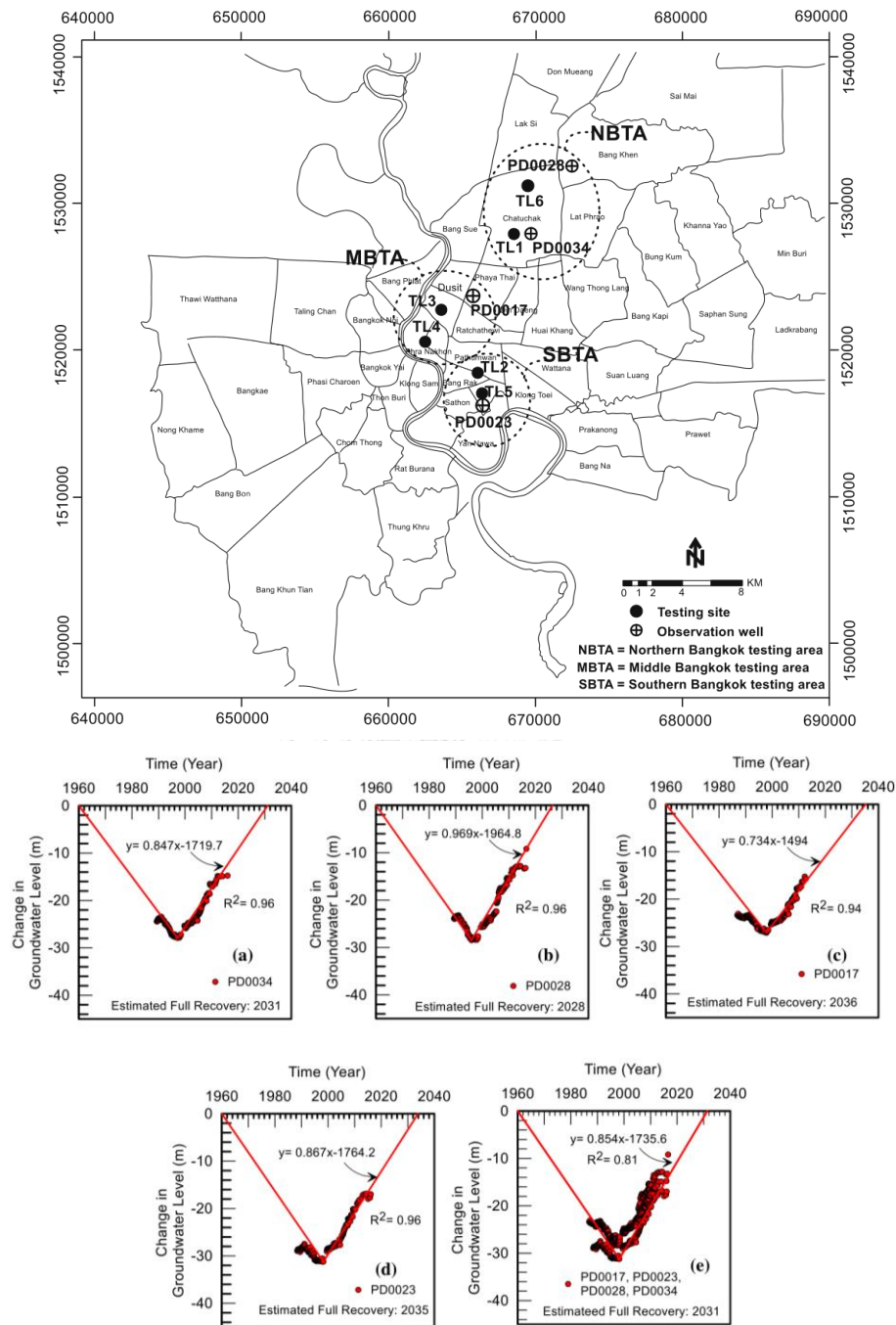
Figure 2-4. Locations of six stations with the change of groundwater level with the period of 1960 to 2040 (Saowiang & Giao, 2020).

Figure 2-5 (a) shows the drawdown of pore water pressure in the period of 1960 to 1997. However, after the restriction of deep well pumping, the groundwater level rebounded as shown in Figure 2-5 (b).
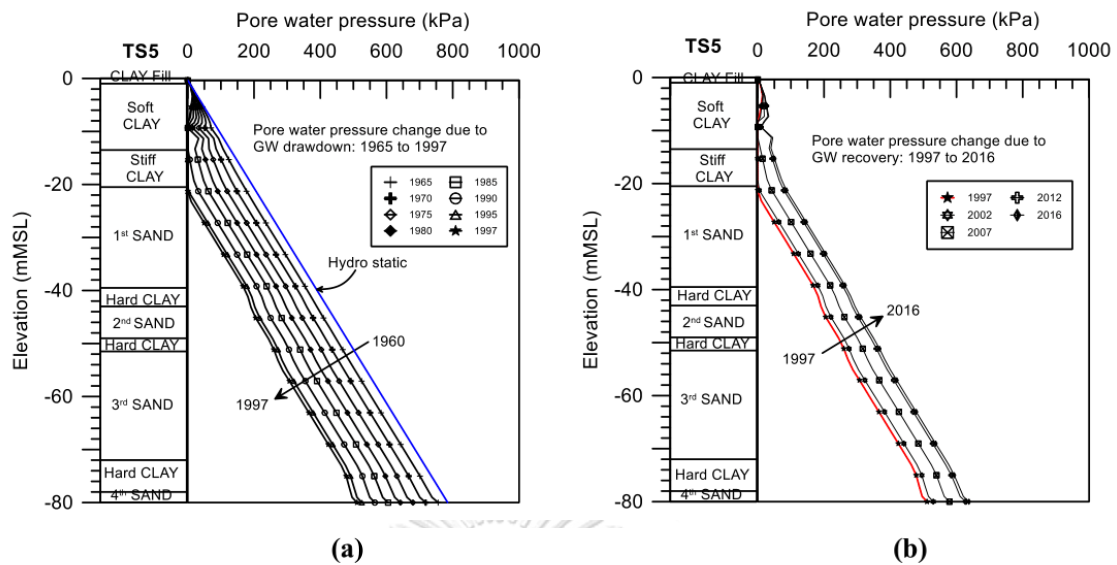
Figure 2-5. The calculated changes in pore water pressure due to groundwater drawdown (a) and recovery (b) for the SBTA site (Saowiang & Giao, 2020)

2.3 Deep Soil Mixing Technique

The deep soil mixing method blends soil with lime or cement to enhance the soil strength. It was introduced in Japan in 1970s. Currently, this technology becomes more popular and used worldwide under various names such as Cement deep mixing (CDM), Deep soil mixing (DSM), Dry jet mixing (DJM) and so on. Deep mixing can be accomplished by wet or dry methods. The equipment for the wet method may have one to eight rotary hollow shafts with cutting tools and mixing blades above the tip. Binder slurry is introduced into the ground through each hollow shaft and exits from nozzles while the shaft penetrates the soil or is withdrawn as shown in Figure 2-6(a). For the dry method, the equipment may have single or dual rotary shafts with cutting tools and mixing blades above the tip and the binder powder is introduced into the ground through each hollow shaft and the nozzle by air pressure, see Figure 2-6(b). The new DM technology, so-called cutter soil mixing, as shown in Figure 2-6(c) breaks soil by cutter wheels and mixes it with cement slurry to produce a homogeneous soil-cement mixture. This technology is most suitable for the construction of cut-off and retaining walls (Han, 2015).
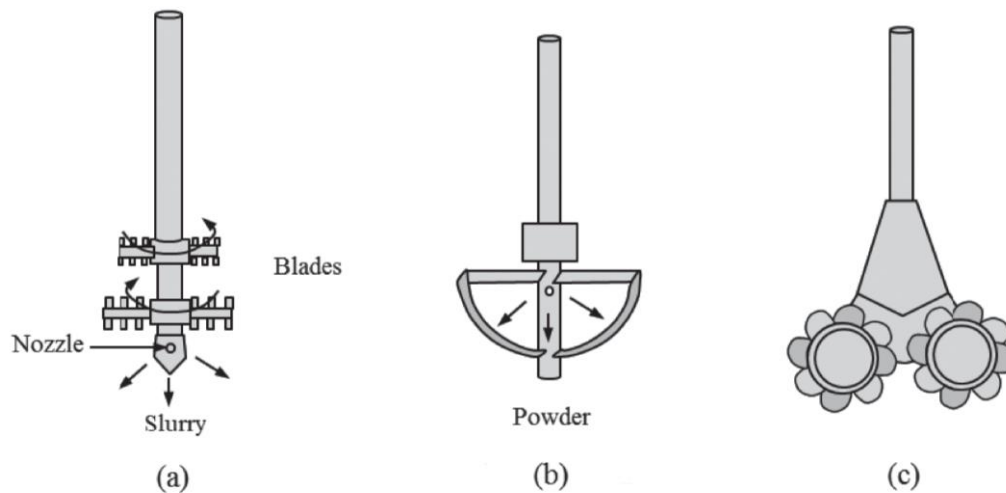
Figure 2-6. Different types of deep mixing techniques: (a) wet method, (b) dry method, (c) cutter soil mixing (Han, 2015).

In Bangkok city, the subsoil is known for Bangkok soft clay which is composed of marine soft clay deposit in the range of 10m – 15m depth. Furthermore, this soft clay is known for high liquid limit which is a huge obstacle in substructure by causing instability and deformation problem. Therefore, deep soil mixing technique in Bangkok is very common for treating the soft soil.

2.3.1 Application of Deep Mixing Technique

The deep soil mixing technique is used in many different applications to modify and solve the various geotechnical problems. Most of the geotechnical problems which deep soil mixing technique is used are:

- Global bearing capacity: soil-cement columns can increase the strength of the soil leading the local and global bearing capacity increase.
- Settlement control: reduce settlement on the soft ground deposit and also reduce the compressibility of natural and placed soils.
- Groundwater control: seepage prevention is created by installing overlapping columns or panels consisting of several connected adjacent columns to intercept the seepage flow path.

- Flow of ground soil-cement columns can provide ground stability and control of ground movements during surface and underground construction such as excavation problem and tunnelling.
- Contamination of groundwater or waste management: since the soil mixing can reduce the permeability of the soil, soil mixing method is used to prevent the groundwater from contamination and also can be used for storing waste.

Furthermore, in the tunnel excavation problems, deep soil mixing method is applied for few conceptions such as the back of the tunnel mirrors for the breakout of retaining wall for maintaining the face stability and stop the seepage of groundwater, and it is applied at the cross-passage to solidify the ground for hand excavation as shown in Figure 2-7 (Hwang, Ju, Tsai, & Fang, 1995). Additionally, in the case of twin tunnels, deep soil mixing method is used to prevent the disturbance of the tunnel which have been completely driving and the minimizing the settlement impact by tunnelling. Sometimes the lining is not installed since the stiffness of soil after treatment is high enough which can be replaced as the low strength concrete.
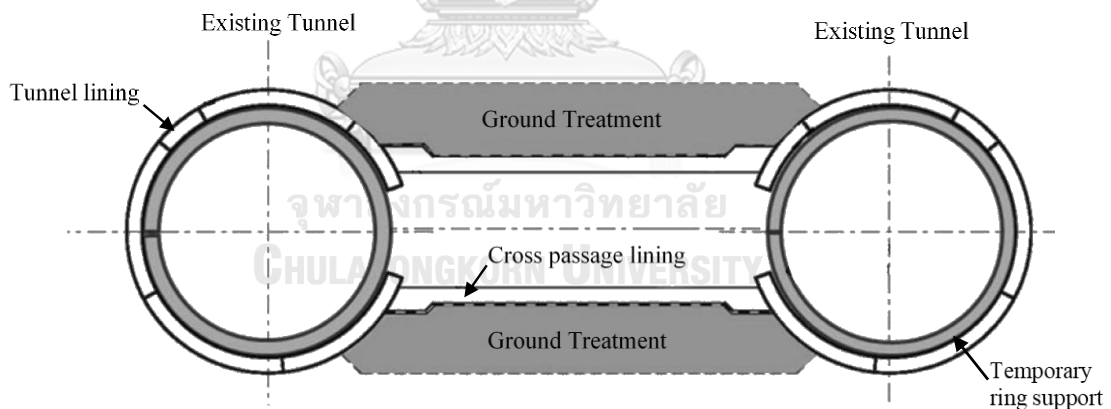
Figure 2-7. Ground treatment of tunnel cross-passage in twin tunnels (Facibeni, 2019)

2.3.2 Types of Pattern

A suitable column installation pattern is chosen considering based on the type, size and importance of the superstructure, the purpose and function of improvement, the construction cost, and the site condition (Kitazume & Terashi, 2013). There are different kinds of pattern in deep soil mixing method: single type, wall type, grid type, and block type (A.Bruce, 2000).
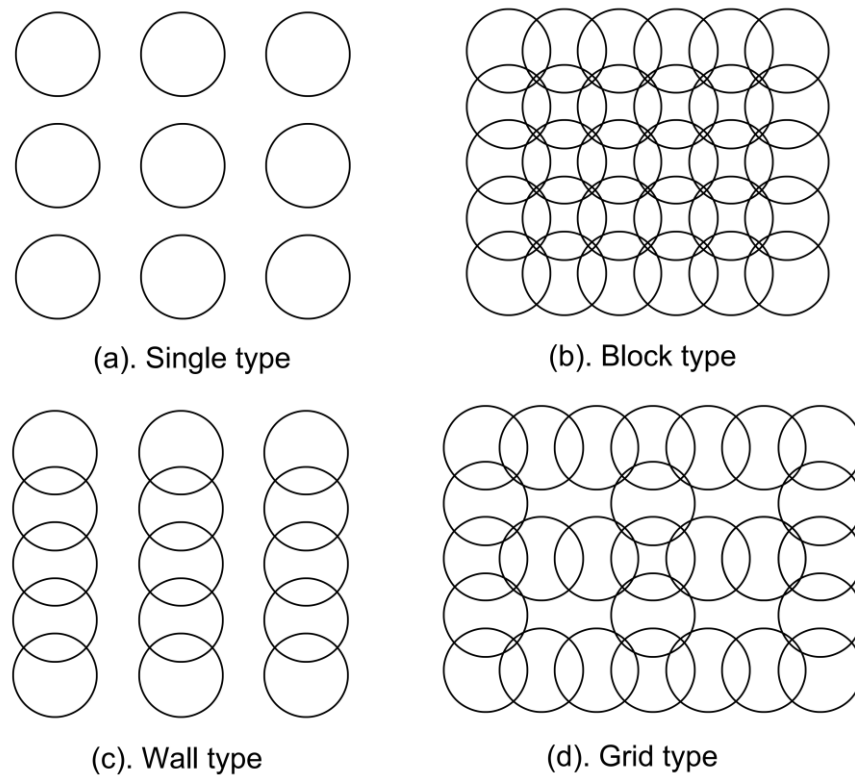
Figure 2-8. Types of the soil-cement mixing pattern in the plan view (A.Bruce, 2000)

2.3.2.1 Single Column Type Improvement

For the single type or group column type improvement, soil-cement columns are separately stabilized in the ground and the volume of improvement is small, Figure 2-9. The area replacement ratio of this improvement pattern is relatively low. This improvement type is mostly used to increase bearing capacity and reduce settlement, for instance, as foundations of embankments or lightweight structures (Kitazume & Terashi, 2013).
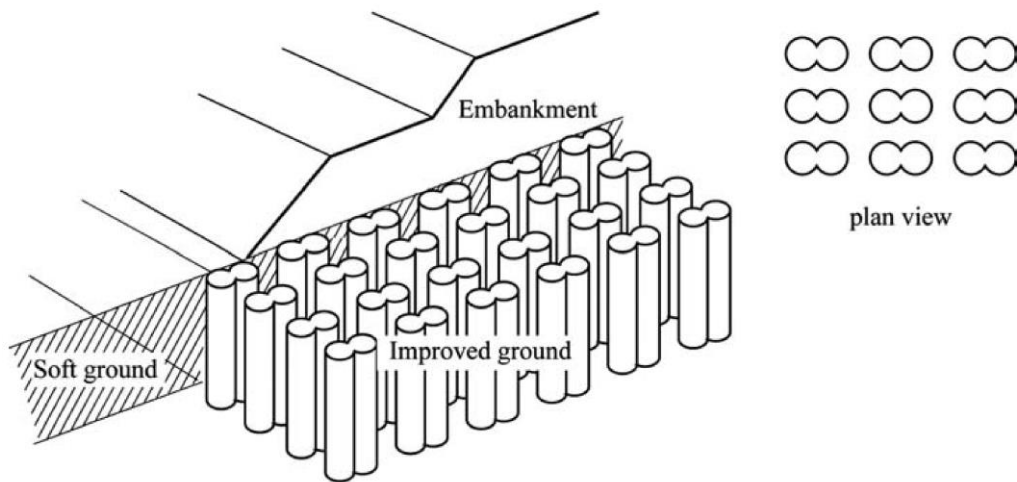
Figure 2-9. Single or group columns type (Kitazume & Terashi, 2013)

2.3.2.2 Wall Type Improvement

For wall type improvement, stabilized soil columns are continuously installed to form reinforcement walls, Figure 2-10. The wall can be used to bear the weight of superstructure and other external loads and transfer them to the deeper stiff layer. The internal stability is affected by wall spacing and depth of the wall. This pattern has been commonly used as a retaining wall for lateral support, a seepage wall to cut off seepage, a curtain wall to contain waste materials, or a wall perpendicular to the centerline of the embankment to increase the stability (Han, 2015; Kitazume & Terashi, 2013).
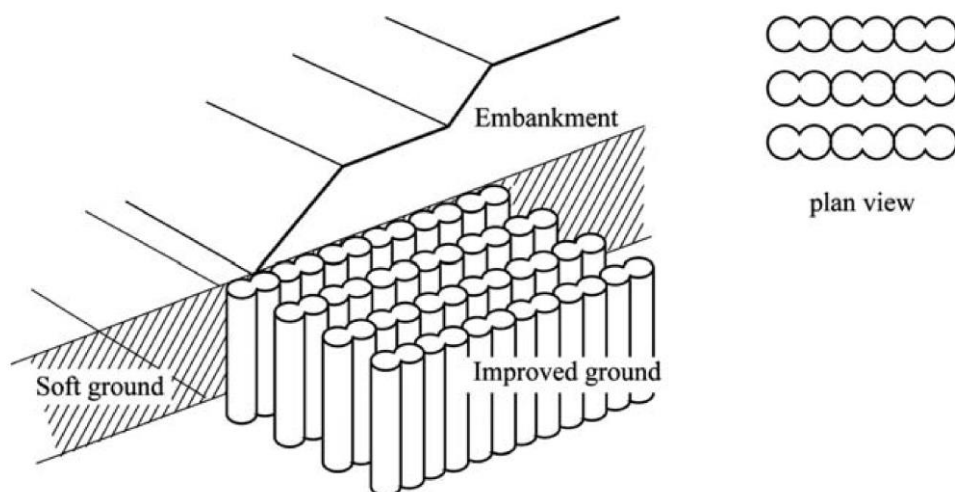
Figure 2-10. Wall type (Kitazume & Terashi, 2013)

2.3.2.3 Grid Type Improvement

The grid-type improvement is an intermediate type between the block type improvement and the wall type improvement. In this pattern, soil columns are installed in overlapping fashion as shown in Figure 2-11. This pattern is highly stable and its cost ranges between the block type and wall type improvements. A unique application of the grid pattern is to mitigate liquefaction of sandy soils since the liquefiable soils are contained inside the grid cells (Han, 2015).
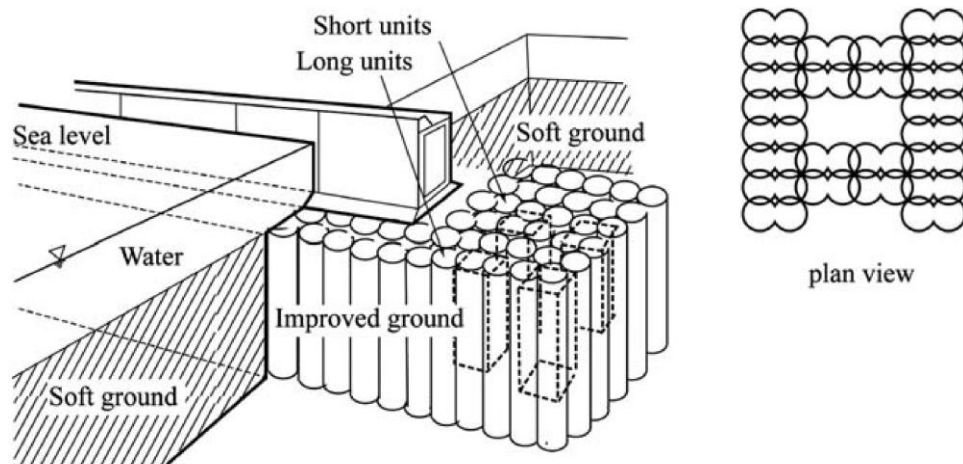
Figure 2-11. Grid type (Kitazume & Terashi, 2013)

2.3.2.4 Block Type Improvement

For block type improvement, all stabilized soil columns are overlapped to forming a large block, Figure 2-12. This improvement is the most stable pattern, but the cost is higher, and the execution period is longer than the other improvement types. This improvement type is mostly used for enhancing the stability of marine constructions and superstructure. It can be used to prevent the leaching of hazardous chemicals (Han, 2015)
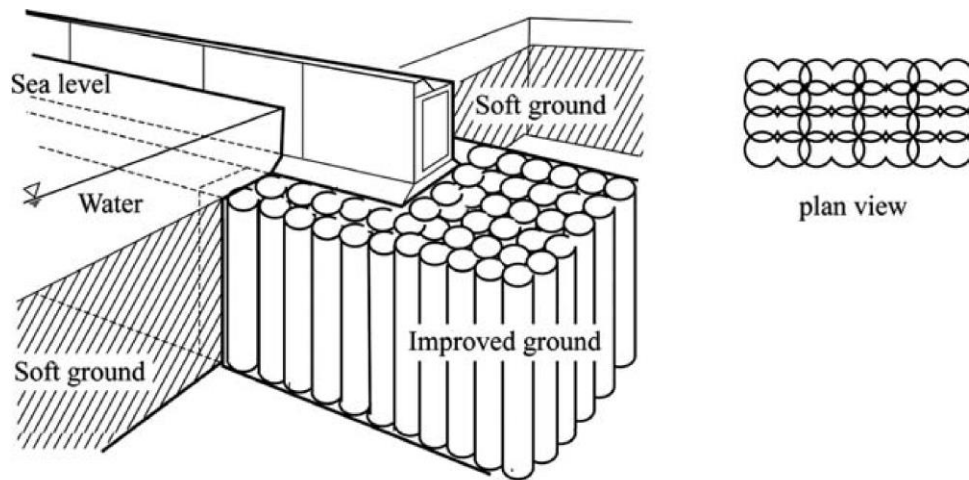
Figure 2-12. Block type (Kitazume & Terashi, 2013)

2.3.3 Replacement Ratio

2.3.3.1 Area Replacement Ratio

For soft soil deposits improved by the inclusion of soil-cement columns, the area replacement ratio (α) is commonly used to describe the relative improvement of the soft layer by the columns. The area replacement ratio was proposed to quantify the amount of soil replaced by soil-cement columns, the term replacement ratio was adopted from Chai and Carter (2011) which was indicated in the Eq (2.1).

$$\alpha = \frac{A_c}{A}$$

(2.1)

where, α = Area replacement ratio

A_c = Cross sectional area of columns

A = Cross-sectional area of ground improvement ($s \times s$)

s = Spacing from the centre to centre of columns

Additionally, the replacement ratio is depending on the pattern arrangement of soil improvement. However, the following Eq (2.1) is using for triangle grid improvement pattern, see Figure 2-13.
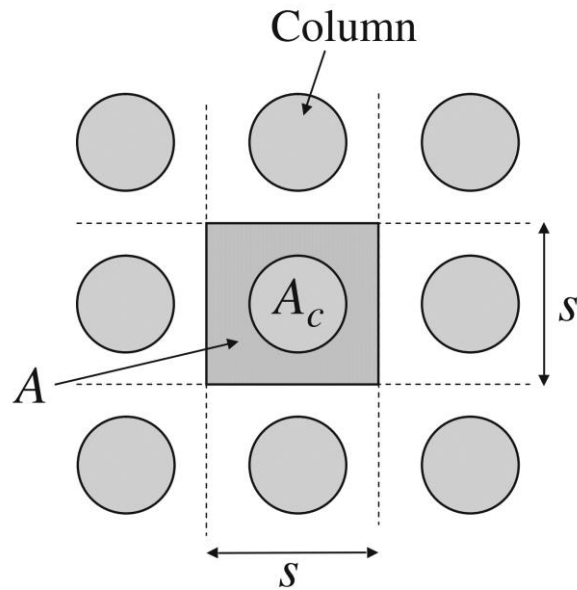
Figure 2-13. Plan view of area replacement ratio (Chai & Carter, 2011)

2.3.3.2 Volume Replacement Ratio

Since the improvement zone was constructed at the underground, the volume ratio is adopted which can be expressed similarly to the area replacement ratio as mentioned in the previous section. The definition of volume replacement ratio can be described as the following equation (2.2) and Figure 2-14.

$$\beta = \frac{V_c}{V} \tag{2.2}$$

where, β = Volume replacement ratio

V_c = Volume of treatment

V = Volume of soil mass ($s \times s \times s$)

Andromalos, Hegazy, and Jasperse (2001) mentioned that the volume replacement ratio is the ratio of the volume of treated soil to the volume of the soil mass.
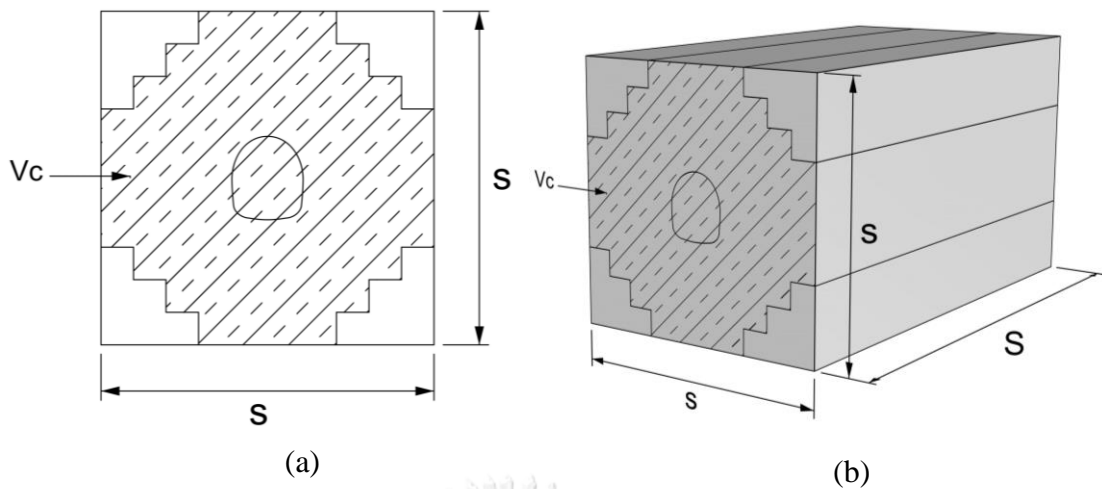
Figure 2-14. (a) Cross-sectional view of treatment soil mass; (b) 3D view of the treated soil mass

2.4 Effect of Soil-cement Column on Soil Strength

Soil-cement is a mixture of cementitious chemical material which is usually referred to as cement, and soils. Cement provides a significant increase in shear strength of soils to meet strength requirements in different applications. The design considerations for the two popular methods which deep soil mixing method (DSM) is for excavation support and vault arch for tunnelling are presented (Fan, Wang, & Qian, 2018).

A research work which is related to deep soil mixing for reinforcing the tunnel and intervention shaft studied on the core samples of unconfined compressive strength tests (UCS) of the DSM column. The results show that the UCS strength of core samples consistently above 1.5MPa after 28 days (Yee & Tan, 2015). However, the strength of the soil-cement columns is not accurate since it is highly affected by many factors such as types of binder, characteristics and conditions of soil, mixing conditions, and curing conditions (Kitazume & Terashi, 2013). For instance, the soil-cement strength of fine-grain soil with high water is lower than that of the soil with low water content (Figure 2-15). For acidic soil conditions, the strength also reduces since the cement reaction is base. Moreover, the duration of mixing and remixing also

affects the strength since the soil and cement need to be mixed to homogenous material.
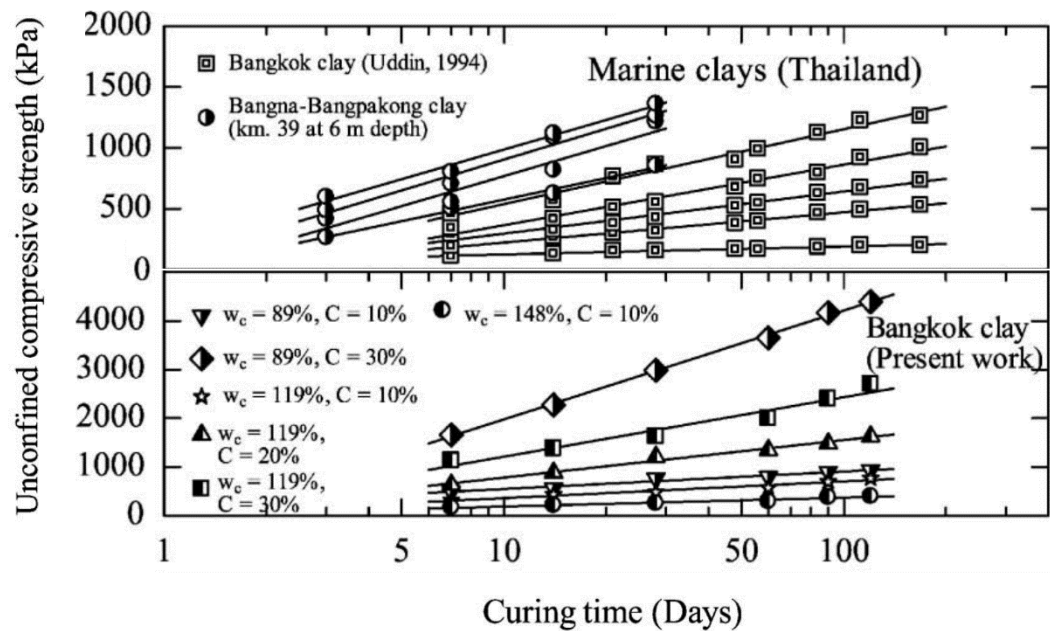
Figure 2-15. Strength development with the time of Bangkok clay (Horpibulsuk, Rachan, Suddeepong, & Chinkulkijniwat, 2011)

The research of strength development of soil-cement in Bangkok clay found that after the soil was improved, there is an increment in the strength of the soil-cement which is up to approximately about 1150 kPa which in the condition of water and cement ratio equal to 1 with 28 days of curing as shown in Figure 2-16. However, Horpibulsuk et al. (2011) proposed that results obtained from laboratory cannot be used since the strength of the soil-cement in the field is less than those obtained from the laboratory. The unconfined compressive strength of soil-cement in field can be calibrated from the unconfined compressive strength of soil-cement determined in laboratory by field strength reduction factor ($q_{uf}/q_{ul} = 0.69$). As shown in Figure 2-16, the strength of soil-cement in field is approximately 800 kPa.
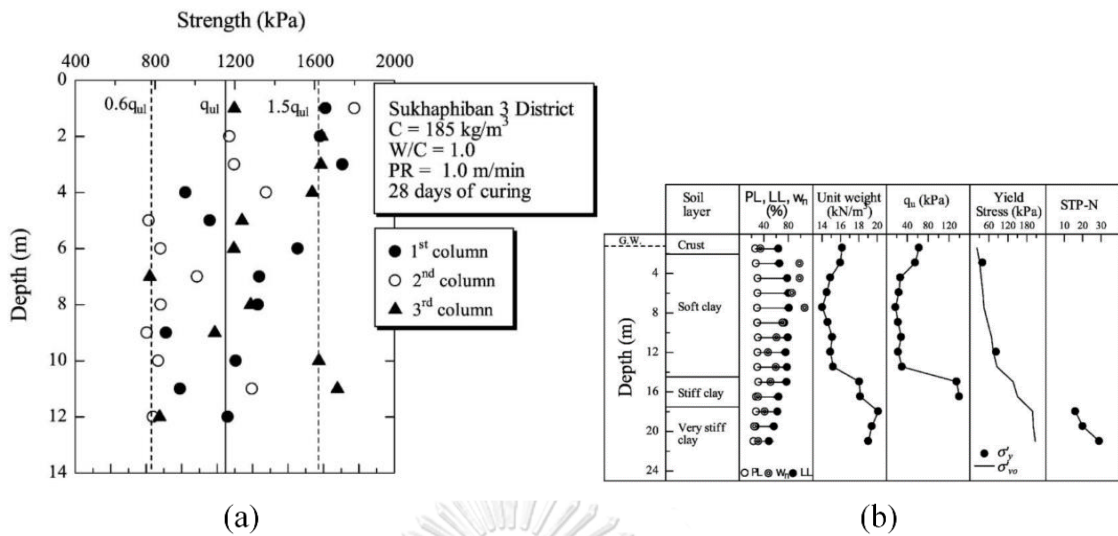
Figure 2-16. (a) Strength profile for soil mixing column at Sukhaphiban 3 district;
(b) Strength of Bangkok subsoil before enhancement (Horpibulsuk et al., 2011)

2.5 Effect of Soil-cement Column Arrangement Pattern

The arrangement pattern of soil-cement column highly affects the stability and cost of soil mixing. The research on optimization of soil mixing and applied to a cross-passage excavation in soft soils and three groups of reinforcement schemes for optimization were analyzed which are (1) all ground layers from the surface to the cross-passage level are reinforced by isolated soil-cement columns (2) block improvement only for the soil layers where the cross-passage sits in and (3) the combination of the umbrella vault technique which either of soi-cement columns in case (1) and case (2) (Wang, Gao, Lee, & Gao, 2014). Wang et al. (2014) found that deep soil mixing is very effective while the umbrella vault shall be used jointly with this technique to enhance the upper soil layers. The optimization of the reinforcing schemes can be evaluated based on the displacement at the crown of the cross-passage and the results show that the cost of soil-cement can be reduced by half from the optimization.
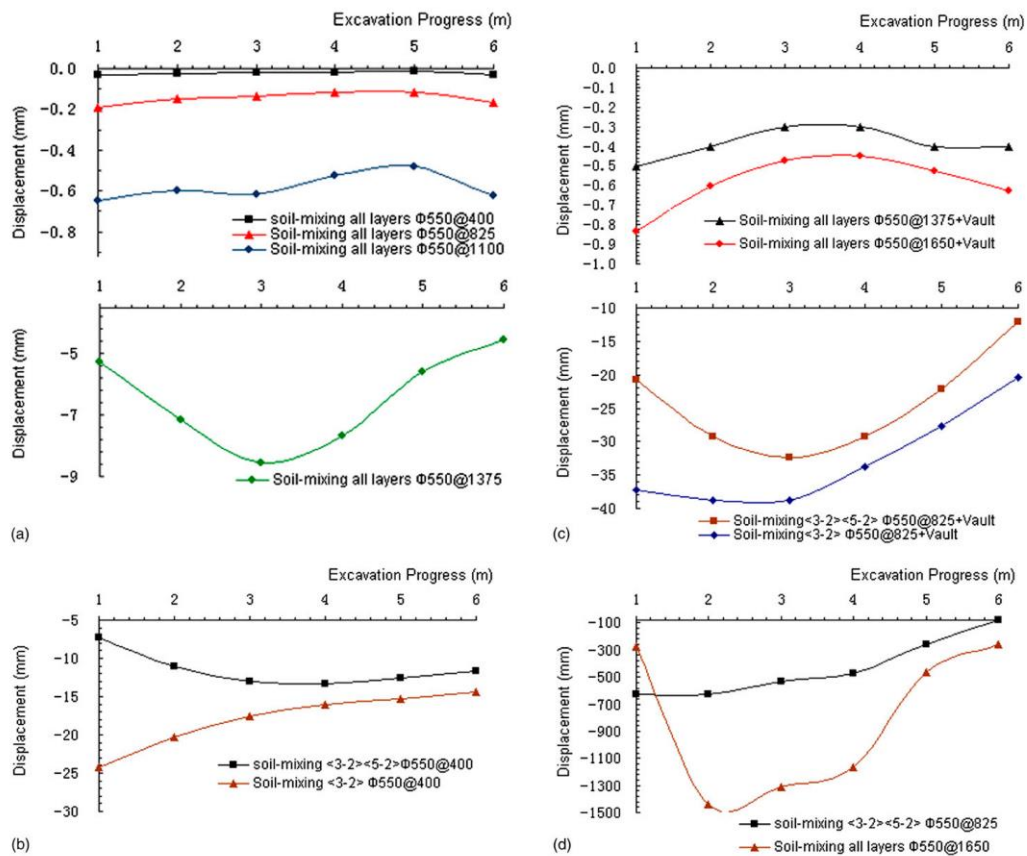
Figure 2-17. Displacements in the longitudinal direction at the crown with the different schemes (Wang et al., 2014).

Figure 2-17 describes modelling results of the settlement at the crown in the longitudinal direction for different optimizing schemes: (a) Displacements at the crown with the different soil-mixing column spacing; (b) displacements at the crown for the cases reinforcing one or two soil layers with deep soil mixing; (c) displacements at the crown for the cases using soil mixing and umbrella vault jointly; (d) unacceptable displacements at the crown. Therefore, using the spacing of 400 mm to reinforce the two layers that the cross-passage sits in would be the best option for 20mm ground surface settlement, which is an acceptable displacement criterion for most applications of metro systems used in China (Wang et al., 2014). However, using the improvement pattern in spacing is not a good choice in case the soil is very soft, tunnel face instability can occur and for seepage reason, the isolated soi-cement column type is not recommended due to lack of interlocking effect.

A research on an embankment reinforced by DSM in Bangkok soft clay showed that soil arching is pronounced when the spacing between rows of DSM column (Sr) is narrow (Sr ≤ 2D). The DSM columns behave as individual isolated columns when the spacing is wide and the soil slides between columns. The optimum spacing was found to be two of DSM column diameter (2D) (Pitthaya Jamsawang, Voottipruex, Boathong, Mairaing, & Horpibulsuk, 2015).

Based on a case study in Kuala Lumpur city, Malaysia, the deep soil mixing (DSM) was designed in block to support an excavation in soft fine-grained soil where intervention shaft and tunnels are constructed. The observed wall movement ranges between 10mm to 15mm which is less than 0.15% of wall height, while the maximum ground settlement are between 2mm and 6mm (Tan, Koo, & Ting, 2019).

2.6 Effect of Undrained Shear Strength on Tunnel Stability

Pressures acting on the face of tunnel excavation plays a crucial rule for maintaining stability. Based on Broms and Bennermark (1967), the tunnel face stability can be justified by the stability ratio (N) defined in Eq (2.3). Since the tunnel face is not sustained by face pressure in the sequential excavation method, the stability is mainly controlled by the undrained shear strength of the ground.

$$N = \left(\sigma_s + \gamma H - \sigma_t \right)/S_u \tag{2.3}$$

where σ_s = surcharge on the ground surface

σ_t = tunnel face pressure

S_u = undrained shear strength

γ = soil unit weight

H = distance from the surface to the tunnel axis

Table 2-1. Tunnel stability ratio of cohesive soil (Peck, 1969; Phienwaja, 1987)

Stability Ratio, N	Tunnel Behavior
1	Stable
2 – 3	Small creep
4 – 5	Creeping, usually slow enough to permit tunnelling
6	May produce general shear failure. Clay likely to invade tail space too quickly to handle.

Additionally, the deep soil mixing method is adopted as a roof barrier for tunnelling. In the case of the TBM driving through a wall of the shaft into the soft soil deposit, the soil around the TBM may decrease its strength due to loosening and trigger off collapsing or settlement owing to the extension of the loosening onto the ground surface, especially in the case of shallowness tunnelling (Shibazaki, 2003). As a result, the design of ground improvement was conducted in the plastic region of the soil where the soil was enhanced by increasing the shear strength. Figure 2-18 (a) shows that when the shear strength was increased, there is no ground failure unless the achieved shear strength touches a failure line of Mohr circle of the original ground. The radial and tangential stress are equal to each other at on the boundary of the elastic region from the plastic region as shown in Figure 2-18 (b) and equation (2.4).

$$\frac{\partial \sigma_r}{\partial r} = \frac{\sigma_\theta - \sigma_r}{r} \tag{2.4}$$

$$\sigma_\theta - \sigma_r = 2C \tag{2.5}$$

where σ_r = radial stress

                    σ_θ = tangential stress

r = variable radius

C = shear strength after improvement
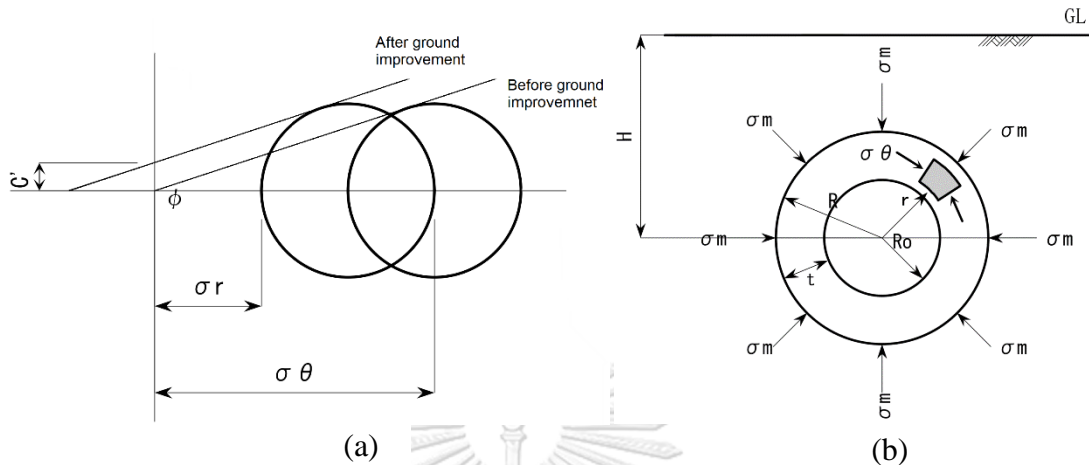
Figure 2-18. (a) Mohr circle of the improved ground and original ground; (b) Cross-section of improvement zone based on the plastic theory (Shibazaki, 2003)

When a tunnel is excavated by the sequential excavation method, a plastic zone will develop around the tunnel. The outer boundary of the plastic zone, or the radius of plastic region, can be determined as followed; (Shibazaki, 2003)

$$\ln R + \frac{R \cdot \gamma_t}{2C} = \frac{H \cdot \gamma_t}{2C} + \ln R_0 \qquad (2.6)$$

where R = radius of plastic region

R_0 = radius of tunnel

γ_t = average unit weight of soil

C = shear strength of improved soil

H = depth to the centre of the tunnel

From equation (2.6), the thickness of the improvement zone can be described as the following equation:

$$t = FS \cdot \left(R - R_0 \right) \tag{2.7}$$

where $\quad$ R = radius of plastic region

R_0 = radius of tunnel

FS = factor of safety

t = thickness of the improvement zone

2.7 Ground Movements Induced by Tunnelling

2.7.1 Ground Settlement

An immediate ground surface settlement profile above a single tunnel can be represented by the normal probability curve or Gaussian distribution (Peck, 1969; Schmidt, 1969):

$$\delta = \delta_{max} \cdot \exp\left(-\frac{x^2}{2i^2} \right) \tag{2.8}$$

where $\quad$ δ = surface settlement at a lateral distance

δ_{max} = maximum surface settlement at the centerline

x = distance from the tunnel centerline

i = distance from the tunnel centerline to inflection point
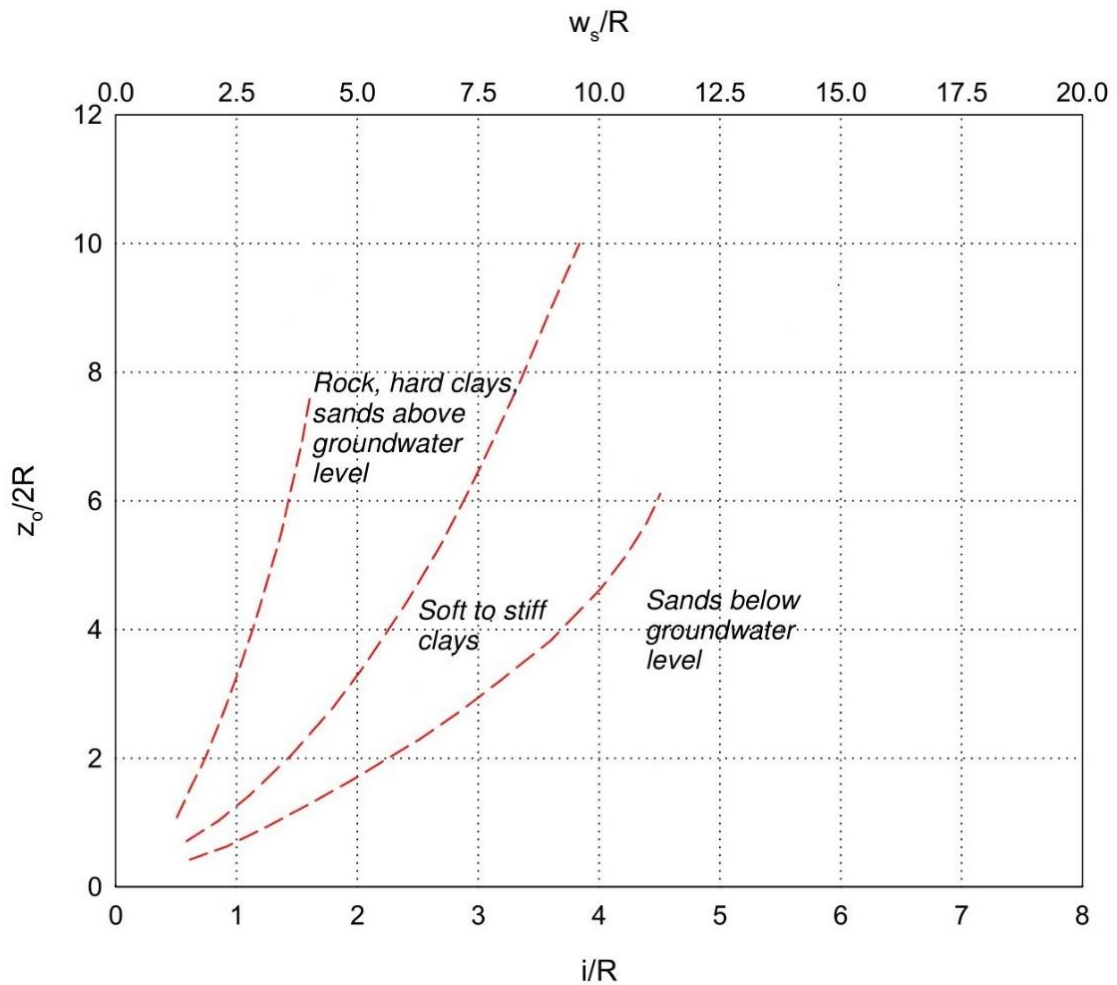
Figure 2-19. Relation between settlement trough, width and tunnel depth for different grounds (Peck, 1969)

O'Reilly and New (1982) proposed empirical equations for estimating the parameter i in eq. **Error! Reference source not found.**) for cohesive soils and granular soils as ollows:

For cohesive soil

$$i = 0.43Z_o + 1.1$$ (2.9)

For granular soil

$$i = 0.28Z_o - 0.1 \qquad (2.10)$$

where i = distance from the centerline

                   Z_o = depth to the tunnel springline

For practical purposes, the parameter i can be approximated by (after O'Reilly & New, 1982)

$$i = KZ_o \qquad (2.11)$$

where i = distance from the tunnel centerline to inflection point

                   K = empirical coefficient

                   Z_o = depth to the tunnel springline

The K value varies with the soil type above a tunnel. O'Reilly and New (1982) suggested that for clays K varies between 0.4 for stiff clay to 0.7 for soft or silty clay. K ranges between 0.2 and 0.3 in the case of granular materials above the groundwater level.

2.7.2 Ground Loss

Ground loss at the ground surface, ΔV_S, is defined by the volume of settlement trough induced by the excavation of a tunnel. The ground loss at the ground surface is approximately same as the contraction of ground around the tunnel after excavated, in other words the ground loss at tunnel ΔV_L. The ground loss at tunnel is caused by various factors including overcut, improper filling of annular space and the extraction rate of ground from the tunnel face. Therefore, ground losses can be categorized in a broad sense as face loss, shield loss, and tail loss.

The face loss can be minimized by providing sufficient face pressure with adequate stand-up time. The shield loss can be minimized by an articulated shield with over

cutters that create small peripheral void space without compromising steering capability around the curve. Minimal tail loss requires a prompt lining installation and an immediate arrest of the annular void behind the tunnel lining. The arrest of the tail void can be accomplished by expanding the lining against the excavation wall or grouting some material behind the lining. From all of this relationship and equation which are indicated in Figure 2-20, the ground loss can be expressed as followed:

$$V_L = \frac{\Delta V_L}{V_o} \tag{2.12}$$

where V_L = volume loss

ΔV_L = volume of tunnel after shrinkage

V_o = initial volume of the tunnel
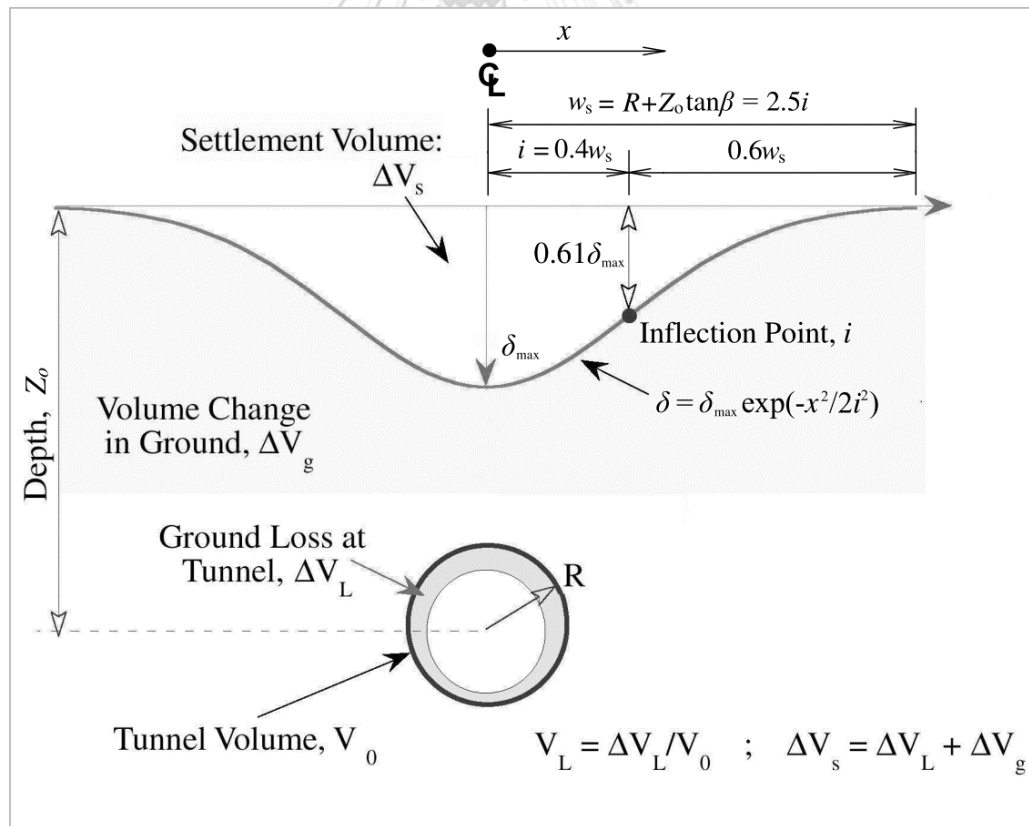
Figure 2-20. Empirical function for transversal surface settlement trough (Peck, 1969)

Ground loss can be estimated by assuming a straight drive, evaluate ground conditions, tunnelling methods, and workmanship (Bickel, Kuesel, & King, 1996) as shown in Table 2-2.

Table 2-2. Estimation of V_L for several representative cases (Bickel et al., 1996)

Case	V_L %
Good practice in firm ground	0.5
• Applies to better soils and excellent ground control	
Good practice in slowly reveling ground	1.5
• Considered good ground	
Fair practice in fast reveling ground	2.5
• More shield and tail loss	
Poor practice in cohesive running ground	4.0 or more
• Yet more shield loss	
• Tail void mostly unfilled by grouting and/or support the expansion of the initial supports	

2.8 Three-dimensional Finite Element Method

With the development of the finite element method, it becomes feasible to analyze and predict the behaviour of soil in geotechnical problems including the ground movement due to tunneling. The finite element analyses in this study are performed in 3D using tetrahedron elements.
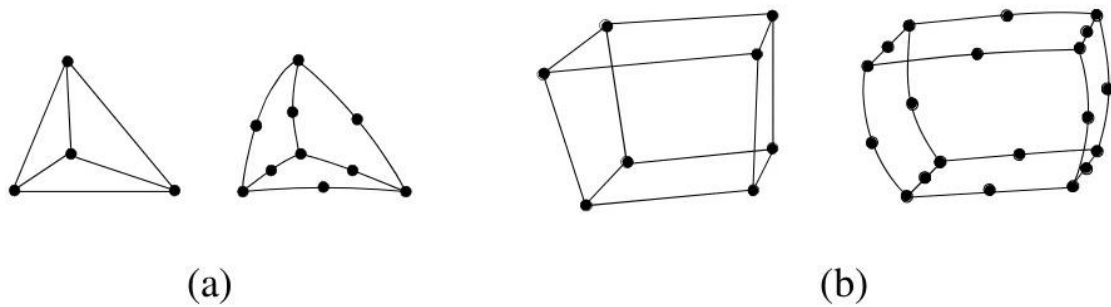
Figure 2-21. 3D finite element mesh for volume element: (a) hexahedron, (b) tetrahedron (Brinkgreve et al., 2016)

2.8.1 Soil Constitutive Modelling

In the urban area, excavation activities have a significant effect on the surrounding area. Therefore, materials behaviour in numerical modelling of geotechnical engineering problems plays a crucial role in predicting the ground movement. A soil constitutive model is a mathematical representation of the behaviour of the soil under load. The model typically relates to the numerical computation between stresses and strains. Schweiger (2009) arranged the constitutive models into 5 groups:

- Linear or nonlinear elastic models
- Elastic-perfectly plastic models
- Isotropic hardening single surface plasticity models
- Isotropic hardening double surface plasticity models
- Kinematic hardening multi-surface plasticity models

2.8.1.1 Mohr-Coulomb Soil Model

Mohr-Coulomb model is also termed as a linear elastic perfectly plastic model. In MCM, the limiting state value of stress method is explained by these parameters: fiction angle (φ), cohesion (c) and angle of dilatancy (ψ) which can be obtained from simple laboratory tests. Moreover, the MCM model only uses one Young's modulus and does not consider the difference between loading and unloading stiffnesses. Hooke's law was endorsed in the elastic zone as shown in Figure 2-22.
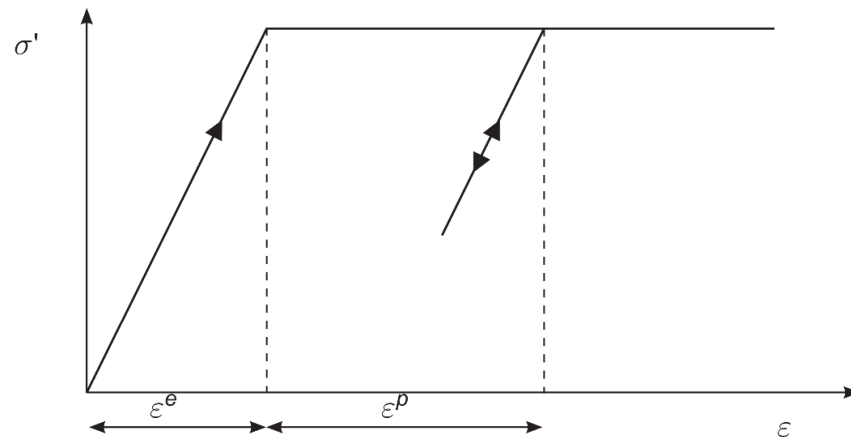
Figure 2-22. Stress-strain relationship of Mohr-coulomb soil model (Brinkgreve et al., 2016)

2.8.1.2 Hardening Soil Model

Hardening soil model (HSM) employs a nonlinear elastic-plastic formulation. The Hardening Soil model is more accurate for predicting wall and ground surface displacements comparing to Mohr-Coulomb model and Modified Cam Clay (Lim, Ou, & Hsieh, 2010). Gaur (2017) and Lim et al. (2010) reported that the prediction by Hardening soil model is more accurate than that of Mohr-coulomb soil model for unloading situation such as the excavation in soft soil.

The HSM employs three stiffness parameters for simulating soil behaviors which are a modulus corresponding to the reference stress (E_{50}), Young's modulus for unloading and reloading (E_{ur}), and oedometer loading stiffness (E_{oed}).

deviatoric stress
$|\sigma_1 - \sigma_3|$
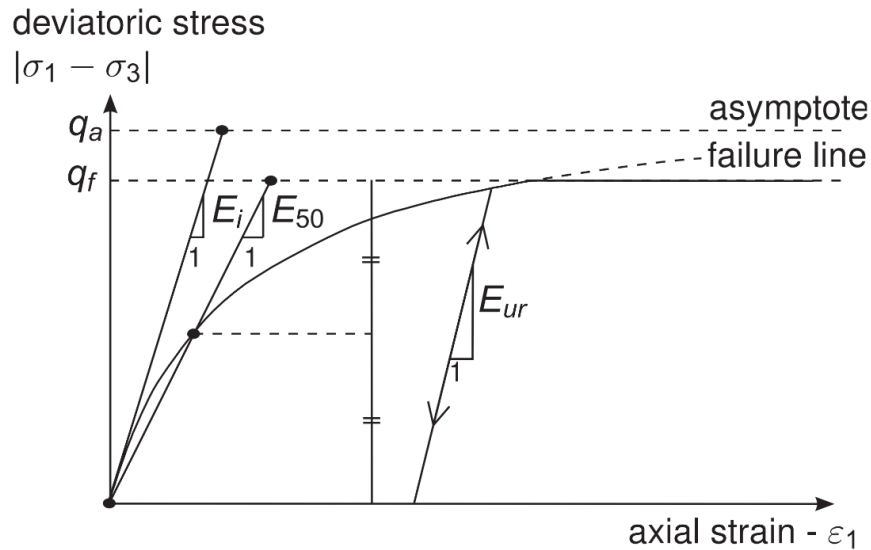
Figure 2-23. Stress-strain relation in primary loading (Schanz, Vermeer, & Bonnier, 1999)

2.8.2 Dimensions of the Finite Element 3D Model

To accomplish the accuracy and minimize computation time, the geometry of FEA mesh were established following the guideline of Möller (2006). For 3D modelling of tunnels with diameter between 4 and 12m, the width of the FEA model can be determined by

$$w = 2D\left(1 + \frac{H}{D}\right) \tag{2.13}$$

where, w = width of mesh generation

H = distance from the ground surface to tunnel crown

D = tunnel diameter

Möller (2006) recommends to provide the distance from the invert of a tunnel to the bottom boundary (h) in the range of (1.1~1.45)×D. Meißner (1996) also propose that the distance to the bottom boundary (h) should be at least (1.5~2.5)×D.
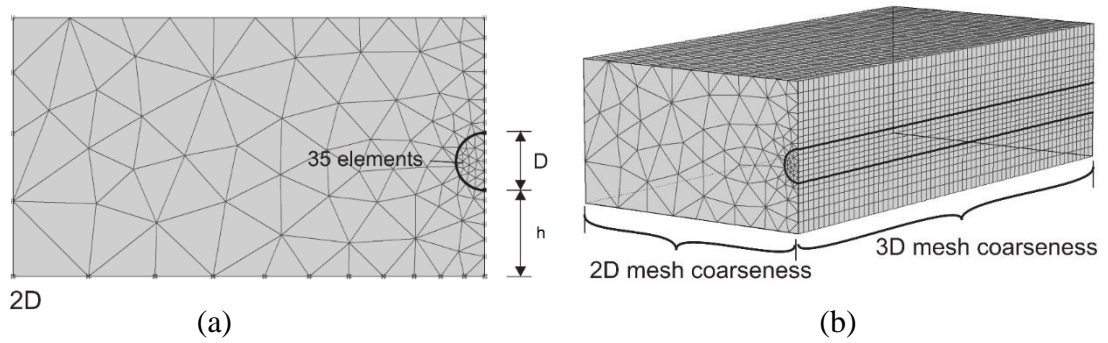
Figure 2-24. (a) Boundary condition in the plan view, (b) Boundary condition of 3D

model (Meißner, 1996; Möller, 2006)

CHAPTER 3
METHODOLOGY

3.1 Pattern Arrangement of Deep Soil Mixing

The arrangement of the deep soil mixing column is determined based on structure types and applications. As mentioned in section 2.3.2, the soil-cement columns can be arranged in four patterns, namely, Single type, Wall type, Grid type, and Block type. The block arrangement was selected in this study since it is safer and suitable for heavy structures and marine clay deposit. The interlocking between columns in all direction also prevents water to flow in the excavated area.
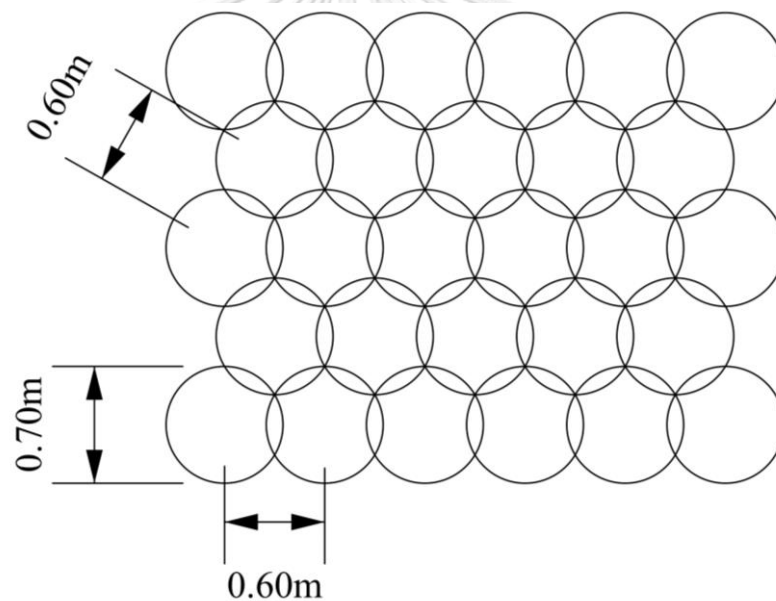
Figure 3-1. Soil-cement columns in block type pattern using in the schemes

3.2 Thickness consideration to prevent seepage

The thickness of the soil cement mixing shall be at least 2m, according to the research in underground oil storage for preventing leakage (Usmani, Kannan, Nanda, & Jain, 2015). As shown in Figure 3-2, the seepage ratio decreases significantly when the thickness is in the range of 0~2.5m and decreases at a slow rate when the thickness is more than 2.5 m. Hence the optimum thickness is around 2.5m.
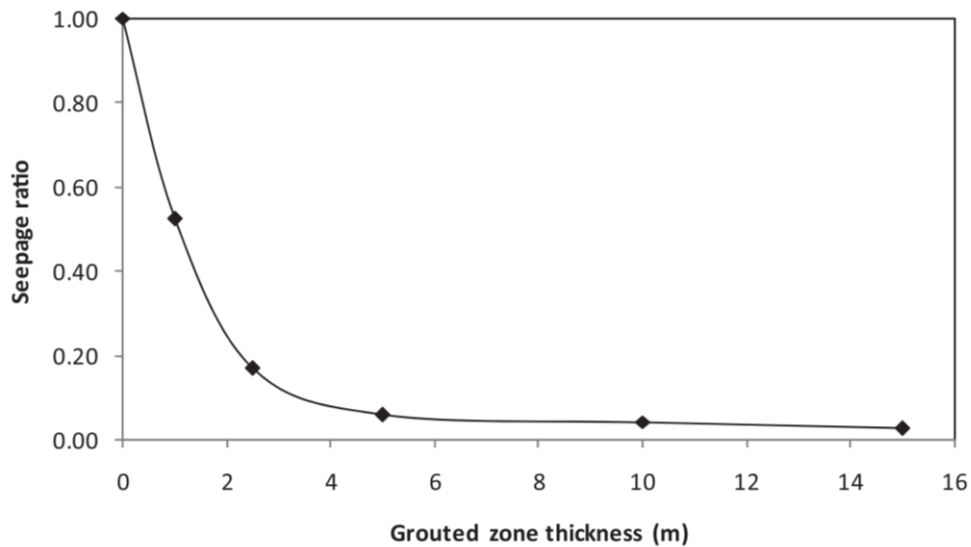
Figure 3-2. Seepage variation along with the grouted zone thickness (Usmani et al., 2015)

Horpibulsuk, Chinkulkijniwat, Cholphatsorn, Suebsuk, and Liu (2012) studied the consolidation behaviour of soil-cement columns in Bangkok by doing the physical model and the finite element model. For the permeability of the soil-cement columns which were used in the finite element is 5×10^{-6} m/min. In actual work, typically, the NATM excavation is between 1m to 3m per day which is depending on ground conditions and tunnel diameter. As a result, for 12m cross-passage, the time spending around 2 weeks. In 2 weeks, for the permeability as Horpibulsuk et al. (2012) mentioned, the groundwater can go through about 0.1m. Hence the ground improvement thickness for preventing short-term seepage problem before the secondary lining installed.

3.3 Optimizing Reinforcement

Mihalis, Konstantis, Vlavianos, and Doulis (2009) proposed that the safety factor of 1.2 and 1.3 can be used for temporary face stability problems and the safety factor of 1.4 or more shall be used for permanent condition. As a result, the safety factor of 1.40 is adopted in this study.

The optimization of improvement volume is conducted by varying the improvement radius (R_i) between 1.2R and 3.0R, as described in Table 3-1. Since the excavation in

this study is not circular, the height of cross-passage is considered in the similar as the diameter of a circular tunnel. For the height of 4.50 m, the diameter D is assumed to be 4.50 m and the radius R is 2.25m (Figure 3-3). In this research, the octagonal section is assumed for ground improvement. However, the outer boundary is slightly modified to be stair-like which better representing the actual state-of-practice.
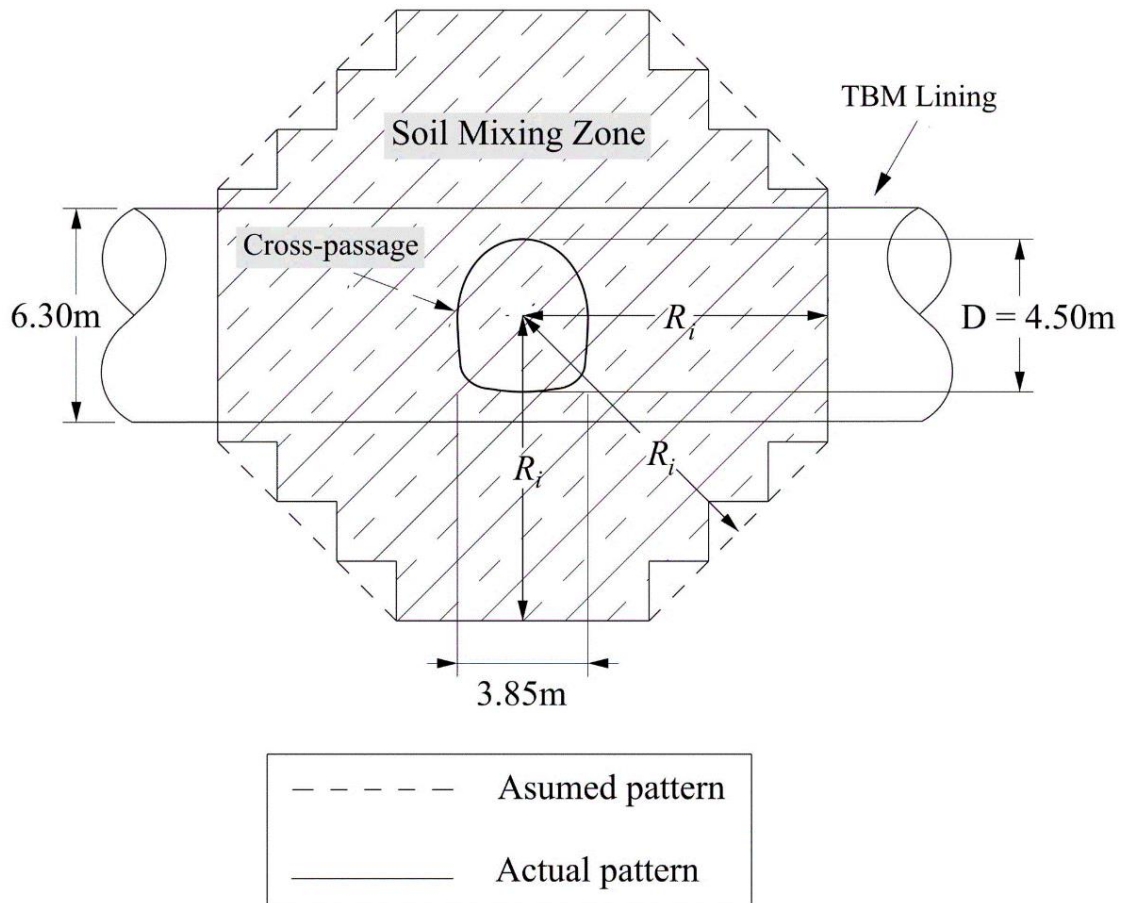
Figure 3-3. Improvement shape in cross-section view

Table 3-1. Radii of ground improvement applied to cross-passage.

Improvement schemes	Improvement Radii (R_i)
1.2R	2.70m
1.4R	3.15m
1.6R	3.60m

1.8R	4.05m
2.0R	4.50m
2.2R	4.95m
2.4R	5.40m
2.6R	5.85m
2.8R	6.30m
3.0R	6.75m

3.4 Simulation of Tunnel Excavation

3.4.1 Model Geometry

Figure 3-4 shows the model geometry which is used in constant level cross-passage. The length, width, and thickness of the model are 80m, 50m and 35m, respectively. Moreover, the model is divided into half for reducing computation time. The model consists of 84,484 nodes and 58,538 elements with the average size of 1.787m. The maximum size of the element is 10.03m while the minimum size of the element is 6.11mm. The model consists of 3 layers as listed below:

- Layer ⟨1⟩ a soft to medium stiff clay layer ranges from the ground surface to 14m depth.
- Layer ⟨2⟩ a stiff clay layer ranges between 14m to 24m depth.
- Layer ⟨3⟩ the first sand layer of Bangkok ranges from 24m to 35 m depth.

Number of elements: 58538
Number of nodes: 84484
Average element size: 1.785m
Max element size: 10.03m
Min element size: 6.114mm
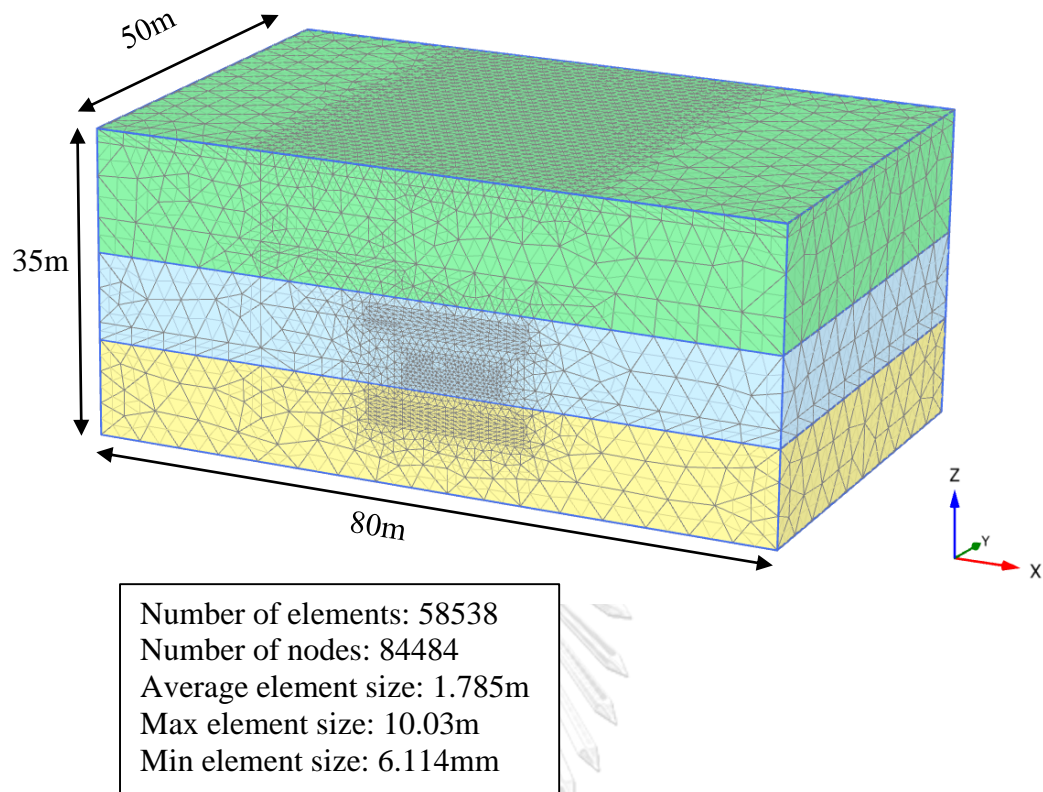
Figure 3-4. Model geometry

3.4.2 Pore Water Pressure Modelling

The pore water pressure is modelled according to Figure 2-5 which is the most updated data. Figure 3-5 shows two groundwater tables used in the model. The first phreatic line is defined at 1.5m depth and the second groundwater table is defined at 10m depth. The pore pressure in the orange zone is interpolated from the defined ground water tables. Figure 3-6 indicated that the simulated pore pressure agrees well with the observed pore water pressure in the literature.
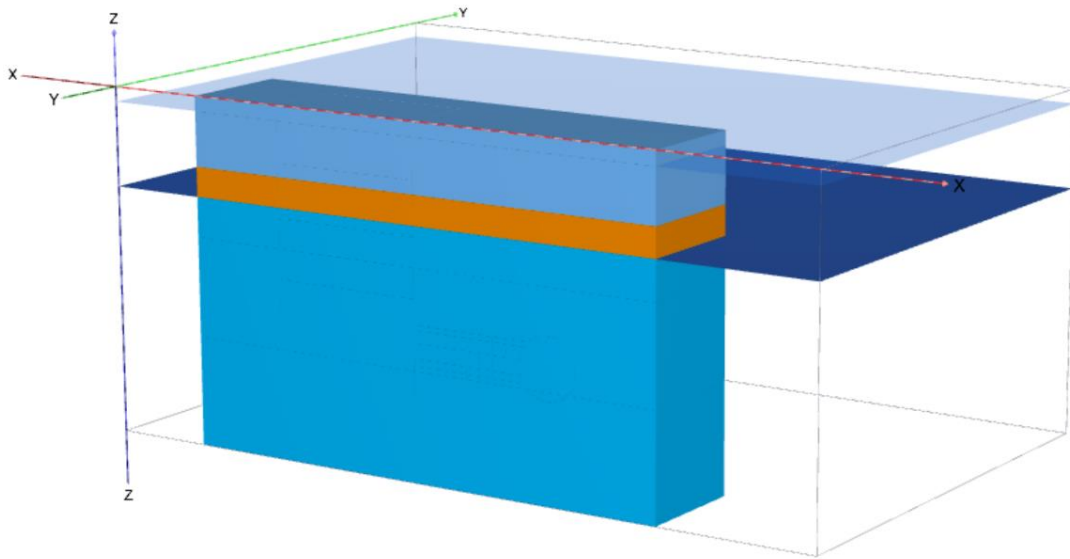
Figure 3-5. Pore water pressure at the initial condition of the 3D model
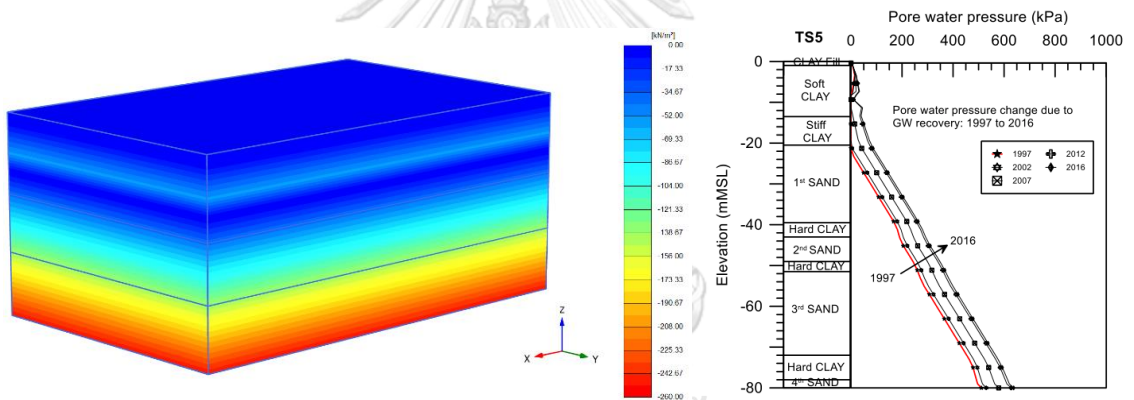
Figure 3-6. Comparing the pore water pressure between 3D modelling and drawdown
pore water pressure graph

3.4.3 Structural Geometry of Finite Element Model
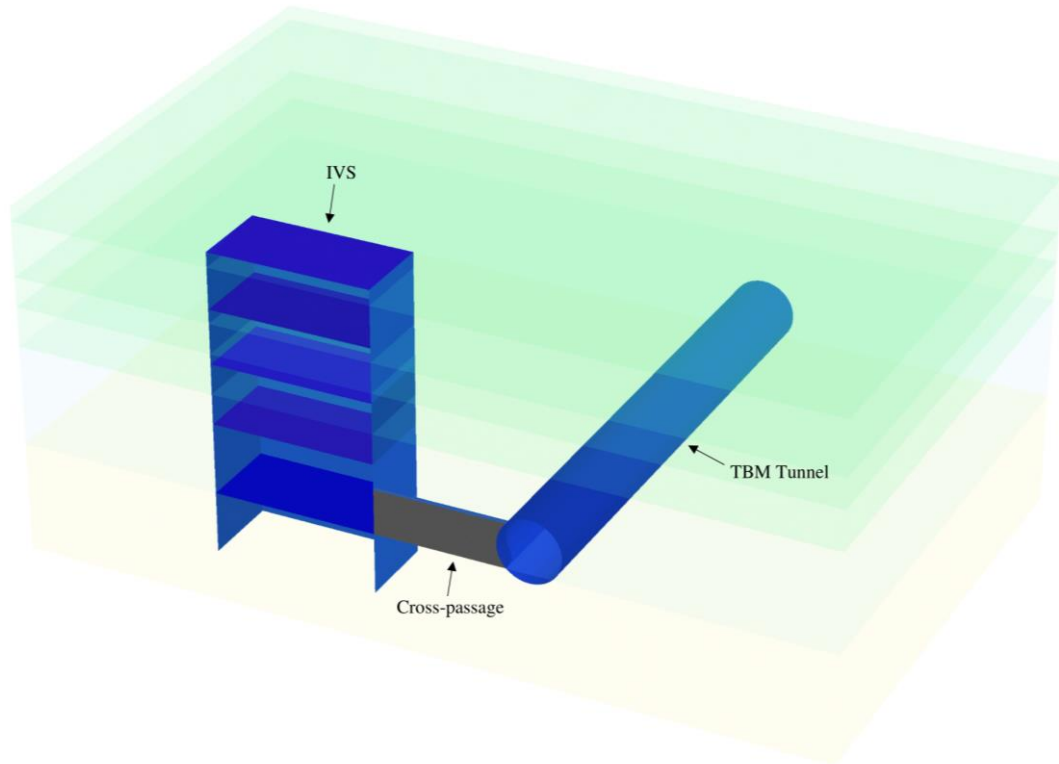
Figure 3-7. Configuration of structures in PLAXIS 3D model

Figure 3-7 shows the structures simulated in the FEA model. The main structural components are a TBM tunnel, the cross-passage and the intervention shaft. Moreover, the IVS is composed of three elements which are D-wall, platform slab and the base slab.

3.4.3.1 Cross-passage Model Geometry

The dimensions of cross-passage and the layout of the model have been illustrated in Figure 3-8 and Figure 3-9. The width and the height of the cross-passage are about 3.85m and 4.5m respectively with the length of 12m. The bottom of the cross-passage was located at -24m from the ground surface (Figure 3-8). The details of the IVS and the TBM tunnel will be described in the next section.
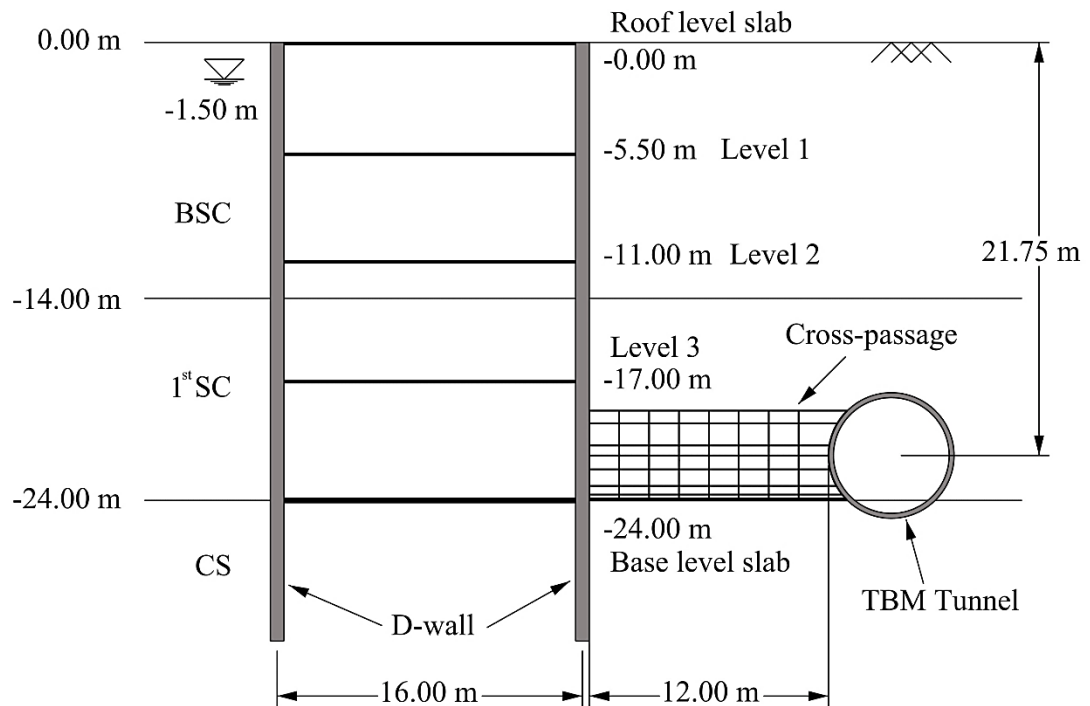
Figure 3-8. Side view dimension of the IVS and cross-passage
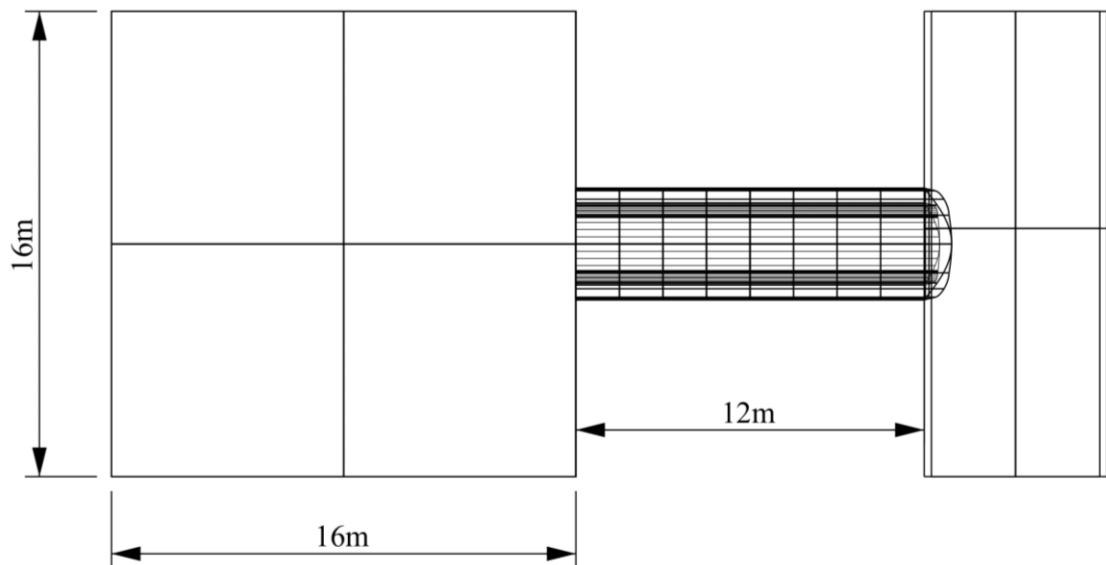
Figure 3-9. Plan view dimension of the IVS and cross-passage

3.4.3.2 Intervention Shaft and TBM Tunnel Model Geometry

The intervention shaft (IVS) is 16m wide by 16m long with 4 basement levels (Figure 3-9). The cross-passage connects to the IVS at the 4th level basement. The TBM

tunnel is modelled based on the ones in Bangkok which has the outer and inner diameters of 6.3m and 5.8m, respectively.

3.4.4 Boundary Condition of Model

Boundary conditions of the FEA are shown in Figure 3-10. The boundary condition of the symmetrical plane was defined as vertical fixity, while the displacements from other direction (u_z and u_x) were free. The upper horizontal boundary has no fixities at all. The displacements were fully fixed in all directions at the bottom plane.
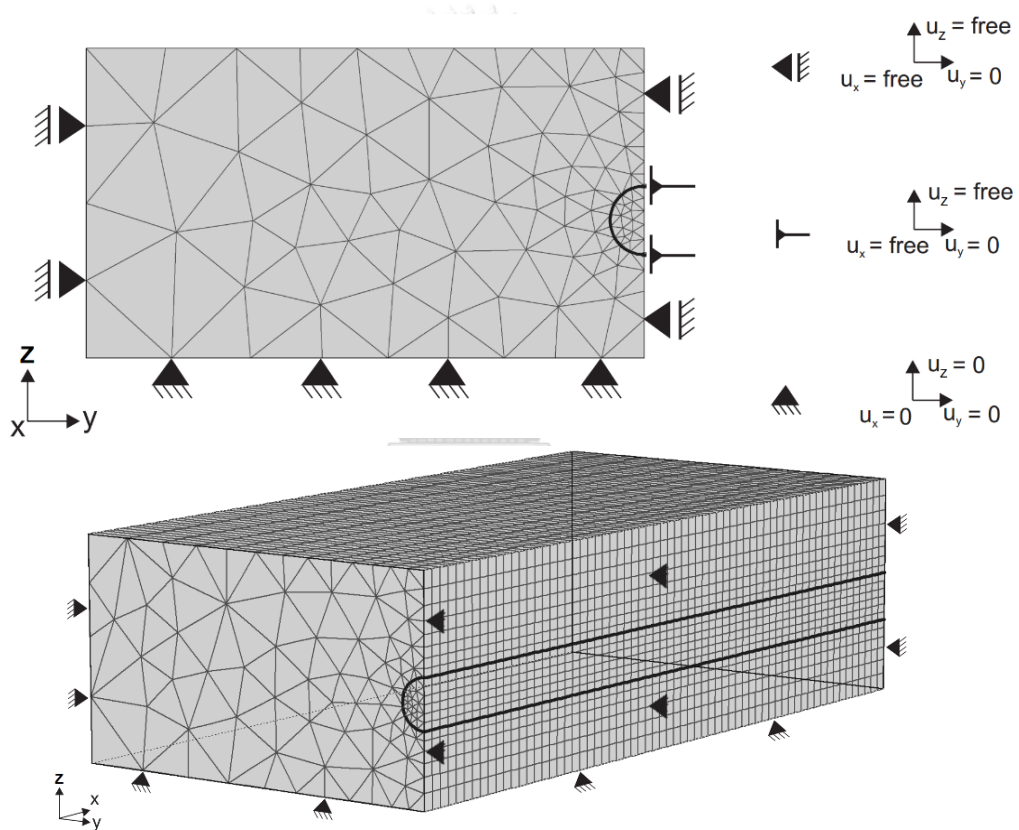
Figure 3-10. Boundary conditions of the bottom, surface and vertical boundaries in the symmetrical half model (Möller, 2006)

3.4.5 Soil Input Parameters

The Hardening soil model has selected this research and the input parameters are adopted from Likitlersuang, Surarak, Wanatowski, Oh, and Balasubramaniam (2013) and shown in Table 3-2.

Table 3-2. Hardening soil parameters (Likitlersuang et al., 2013)

Layer	Soil Type	γ_b (kN/m³)	c' (kPa)	ϕ' (°)	ψ' (°)	E_{50}^{ref} (MPa)	E_{oed}^{ref} (MPa)	E_{ur}^{ref} (MPa)	ν_{ur}	m	K	R_f	Analysis Type
1	BSC	16.5	1	23	0	0.8	0.85	8.0	0.2	1	0.7	0.9	Undrained (A)
2	1st SC	19.5	25	26	0	8.5	9.0	30.0	0.2	1	0.5	0.9	Undrained (A)
3	CS	19	1	27	0	38.0	38.0	115.0	0.2	0.5	0.55	0.9	Drained

3.4.6 Structural Material Modelling Parameters

In this study, the structural materials to be modelled are tunnel lining and intervention shaft. The TBM lining and the IVS are modelled by plate elements. The parameters of the plates are adopted from Lueprasert, Jongpradist, Charoenpak, Chaipanna, and Suwansawat (2015) and Chheng and Likitlersuang (2018) and summarized in Table 3-3

Table 3-3. Parameters of the tunnel, cross-passage lining and intervention shaft (Lueprasert et al., 2015) and (Chheng & Likitlersuang, 2018)

Parameters	d (m)	γ (kN/m^3)	E (GPa)	v	Type of element
Tunnel lining	0.30	24	31	0.2	Plate element
D-wall	1.00	16.5	28	0.15	Plate element
Slab	1.00	25	28	0.15	Plate element
Base slab	1.80	25	28	0.15	Plate element

3.4.7 Soil-cement Parametric Studies

Soil-cement mixture can be considered as poor concrete with low unconfined compressive strength. The soil-cement is modelled by the Mohr-coulomb soil model. The input parameters were adopted from Pitthaya Jamsawang, Yoobanpot, Thanasisathit, Voottipruex, & Jongpradist (2016) as shown in Table 3-4.The strength of soil-cement is about 800kPa based on cored samples from field (Pittaya Jamsawang, Bergado, & Voottipruex, 2011). Based on literatures in Thailand, the Young's modulus of soil-cement value is in the range of 77 to 91 MPa. In this study, Young's modulus is assumed to be 80 MPa based on empirical formula shown in Table 3-5 ($E_{\text{soil-cement}} = 101qu$),

Table 3-4. Soil-cement parameters (Pitthaya Jamsawang et al., 2016)

Material Type	Analysis Type	v	γ_b (kN/m³)	c (kPa)	E (MPa)
Soil-cement	Undrained (B)	0.33	15	400	80

Table 3-5. Relationship between young's modulus and unconfined compressive strength in the DSM (Alipour, Khazaei, Pakbaz, & Ghalandarzadeh, 2017)

Researcher	Location	Relationship
(Topolnicki & Pandrea, 2012)	Europe	$E_{\text{soil-cement}} = 380qu$
(Filz, Adams, Navin, & Templeton, 2012)	USA	$E_{\text{soil-cement}} = 300qu$
(Kitazume & Terashi, 2013)	Japan	$E_{\text{soil-cement}} = (350 - 1000)qu$
(Pitthaya Jamsawang et al., 2016)	Thailand	$E_{\text{soil-cement}} = 101qu$
(Alipour et al., 2017)	Iran	$E_{\text{soil-cement}} = 115qu$

3.4.8 Excavation Sequences

The new Austrian tunnelling method (NATM) was developed soon after World War II after then It has been improved by Mueller, Rabcewicz, Brunner and Pacher. Certainly, this method is well-known for its success in a variety of conditions ranging from hard to soft rock, soft stable ground to weak, friable and unstable ground. Especially it has been successfully used in urban areas, particularly under some major cities, to construct underground facilities (Tatiya, 2017).
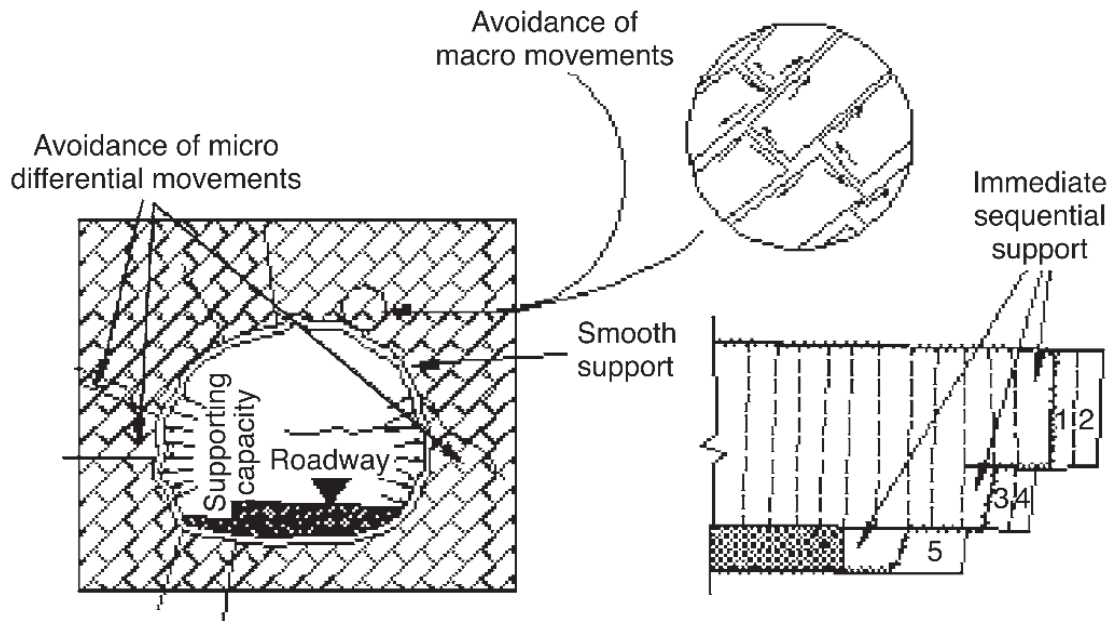
Figure 3-11. The sequential support to prevent micro and macro differential movements of the NATM (Tan et al., 2019)

The tunnel cross-passage of this simulation was simulated in stage following the sequential excavation method. Firstly, the intervention shaft (IVS) was constructed. Then, soil-cement mixing columns were conducted in the cross-passage area. Then the TBM tunnel which will be connected to the cross-passage was constructed. After the TBM, IVS and the soil-cement mixing were completed, the excavation for tunnel cross-passage was started. Firstly, the cross-passage face was opened and the soil was excavated forward in 1.5 m steps until reaching the IVS. The construction sequences are tabulated in **Error! Not a valid bookmark self-reference.** and illustrated in Figure 3-12 from (a) to (f).

Table 3-6. Calculation phase in 3D FEM Plaxis

Phase no.	Phase name	Loading input	Activity simulated
0	Initial phase	K0 stress	Initial condition
1	Intervention Shaft	Construction stage	The shaft is activated and deactivated the soil cluster inside

			shaft while removing water.
2	Soil mixing	Construction stage	Soil treatment was assigned.
3	Tunnel	Construction stage	The tunnel is activated and deactivated the soil cluster inside the tunnel while removing water
4	Cross-passage	Construction stage	The excavation is conducted step by step in every 1.5m. Moreover, the displacement is reset to zero.
5	Safety Factor	Phi-C reduction	Reset displacement to zero.

จุฬาลงกรณ์มหาวิทยาลัย
CHULALONGKORN UNIVERSITY
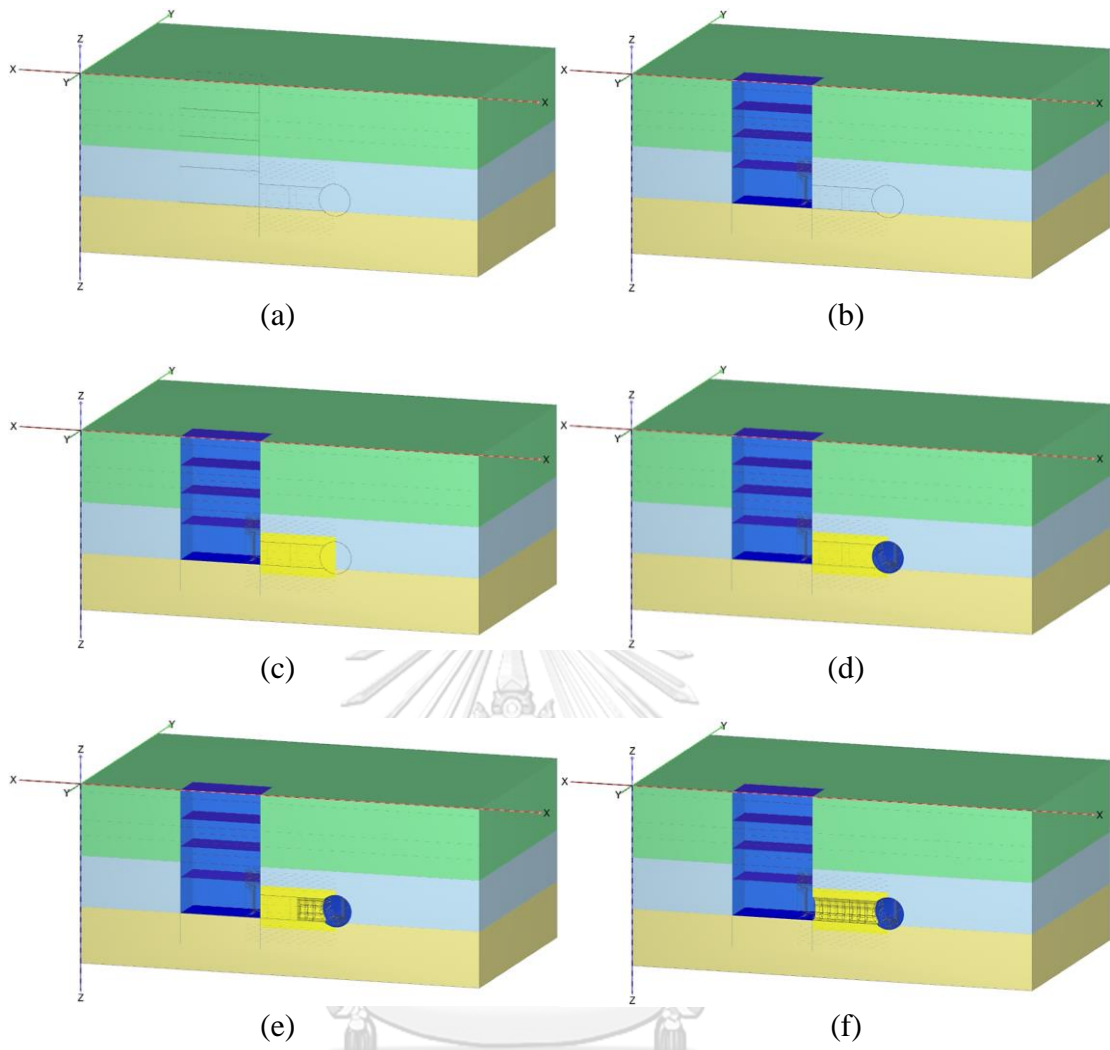
Figure 3-12. The Process of Cross-passage in PLAXIS 3D: (a) Initial Phase, (b) Activate the IVS, (c) Activate Soil-cement block, (d) Activate the TBM tunnel, (e) Cross-passage face opening and excavation, (f) Final excavation

CHAPTER 4
RESULTS AND DISCUSSION

4.1 Stability of Cross-passage

Figure 4-1 shows the safety factor which increases linearly with the improvement thickness. The round marks denoted FEA results while the triangle marks denoted values determined by the plastic theory (Shibazaki, 2003). The discrepancy between two methods increases as the improvement radius decreases. It is noted that the analytical formula of Shibazaki (2003) was based on circular improvement shape while the octagonal shape is employed in this study.
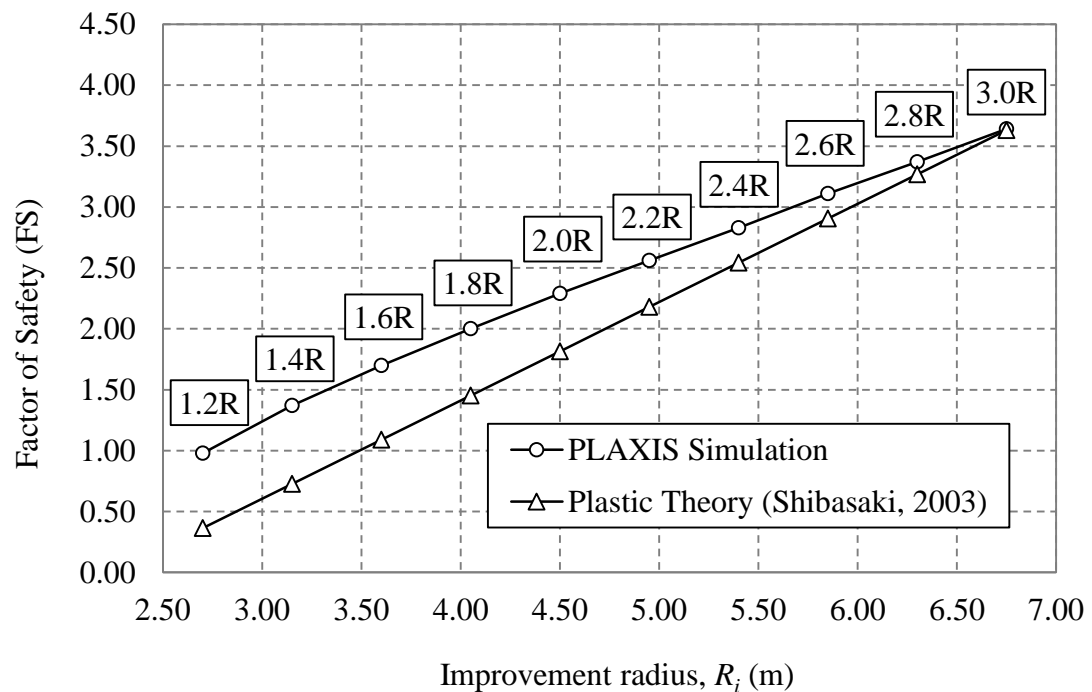
Figure 4-1. Stability of the cross-passage

From the graph, the safety factor of the 1.6R case is 1.7 which is more than 1.40. The thickness of the ground improvement of this case is about 1.35m which is more than 0.1m required for preventing short-term seepage problems. The safety factor of 1.4R scheme is 1.37 which is less than 1.4; however, in case of temporary support, the improvement scheme of 1.4R can be considered. Improvement scheme 1.2R shows

that the safety factor is less than 1. From the simulation, the cross-passage collapsed at the 4.5m excavation.

4.2 Behaviour of Ground Displacement

The 3D finite element analysis provides the results of the ground behaviour of the improved soil with the improvement radius increased from 1.2R to 3.0R. The maximum vertical settlement of 1.2R improvement scheme is about 37.22mm while the settlement decreases significantly to less than 1.5mm in 3.0R scheme, see Figure 4-2 and Figure 4-3. The improvement scheme of 1.2R and 1.4R show that the vertical displacement is very large which are about 10 times of those shown in Figure 4-3.
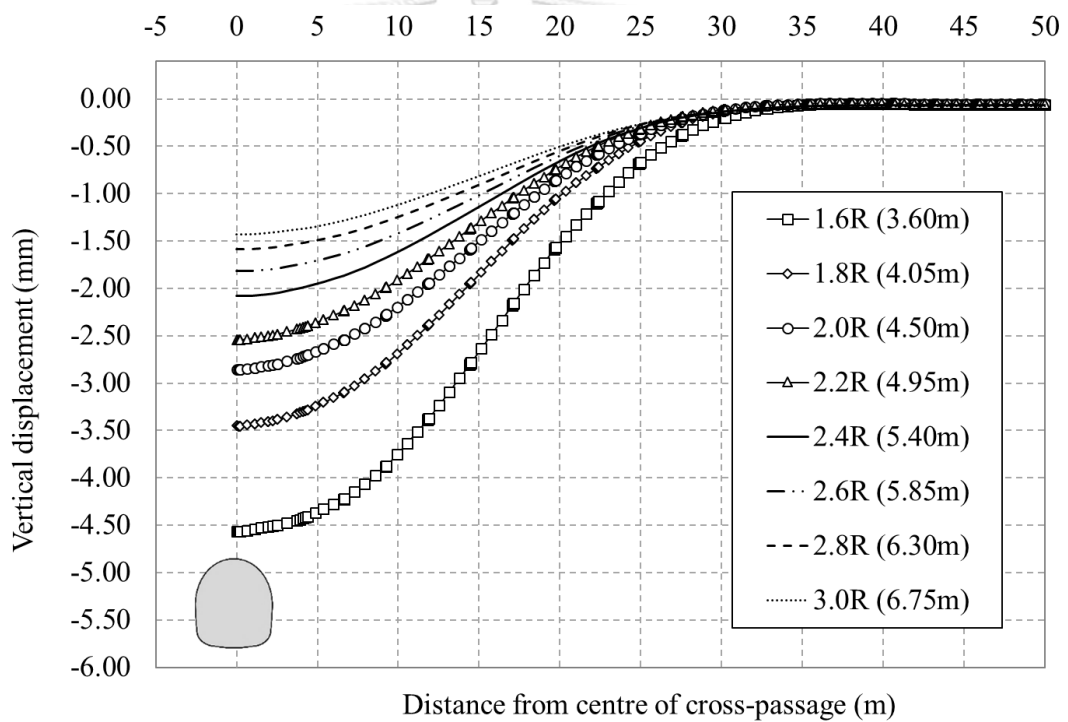
Figure 4-2. Comparing the surface settlement of 1.6R to 3.0R improvement schemes
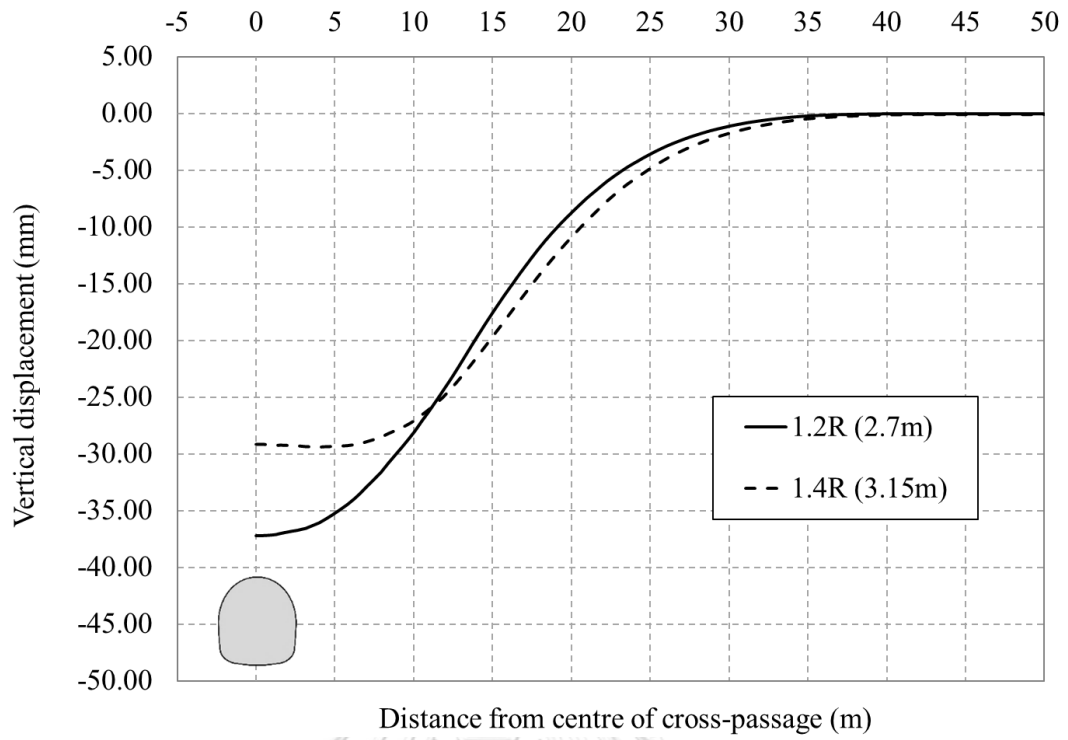
Figure 4-3. Comparing the surface settlement of 1.2R and 1.4R schemes

(a)

(b)

(c)

(d)

(e)

(f)

(g)

(h)

(i)

(j)
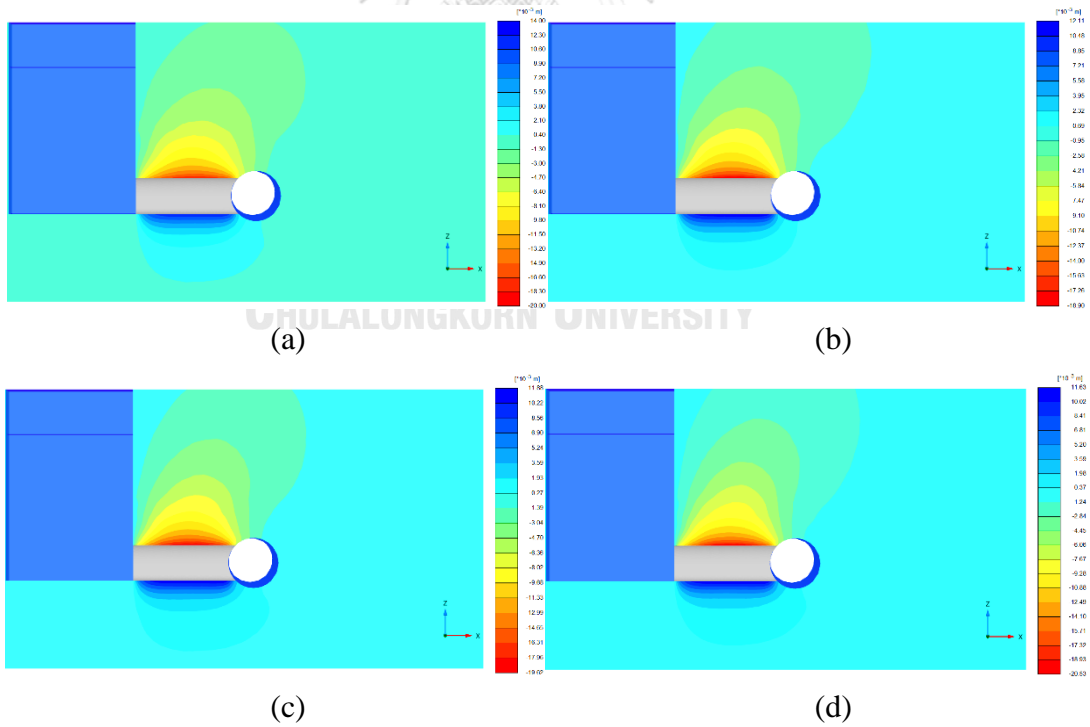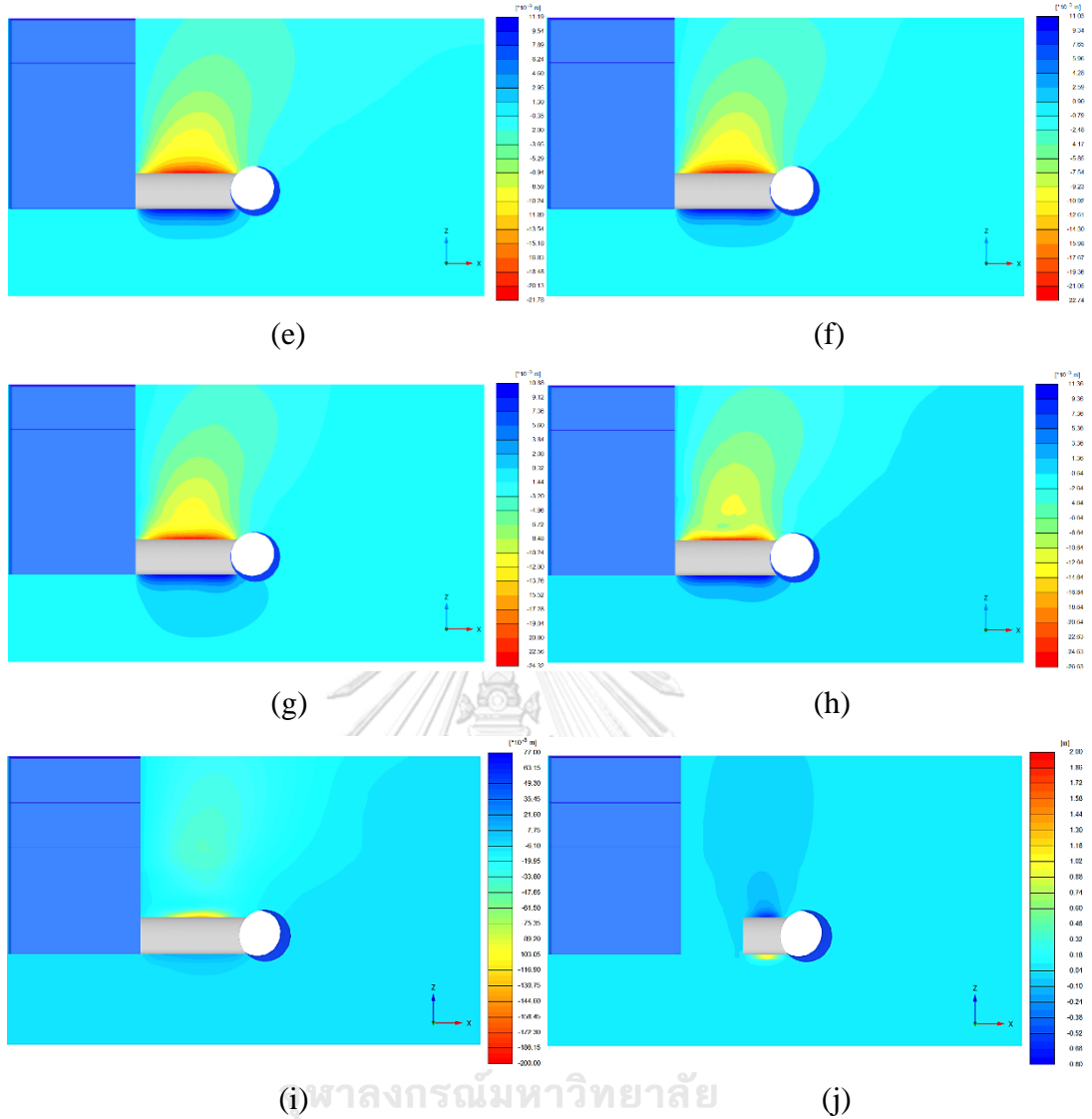
Figure 4-4. Vertical displacement of 3D FEA on cross-passage final excavation stage in different ground improvement thickness schemes: (a) 3.0R; (b) 2.8R; (c) 2.6R; (d) 2.4R; (e) 2.2R; (f) 2.0R; (g) 1.8R; (h) 1.6R; (i) 1.4R; (j) 1.2R

(a)

(b)

(c)

(d)

(e)

(f)

(g)

(h)
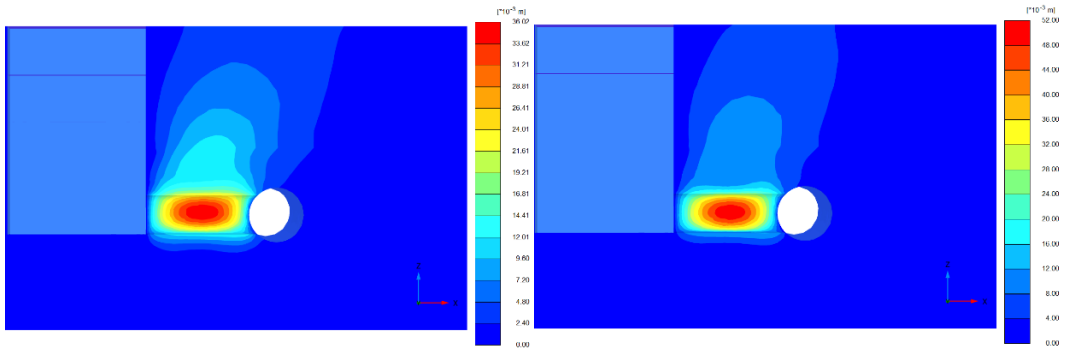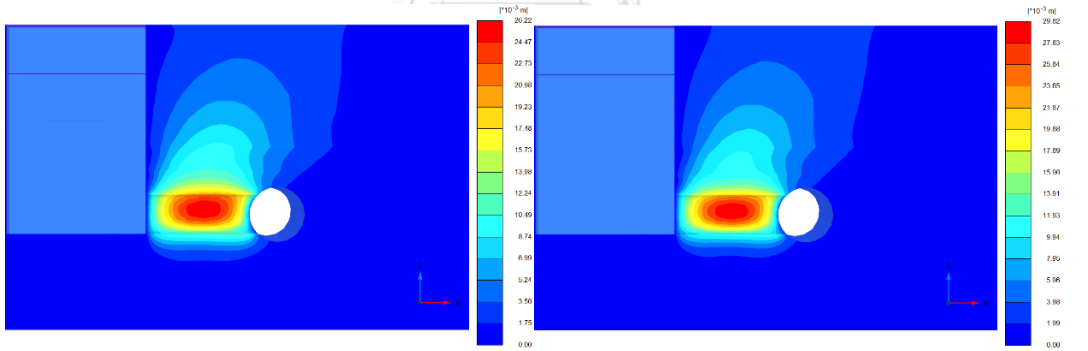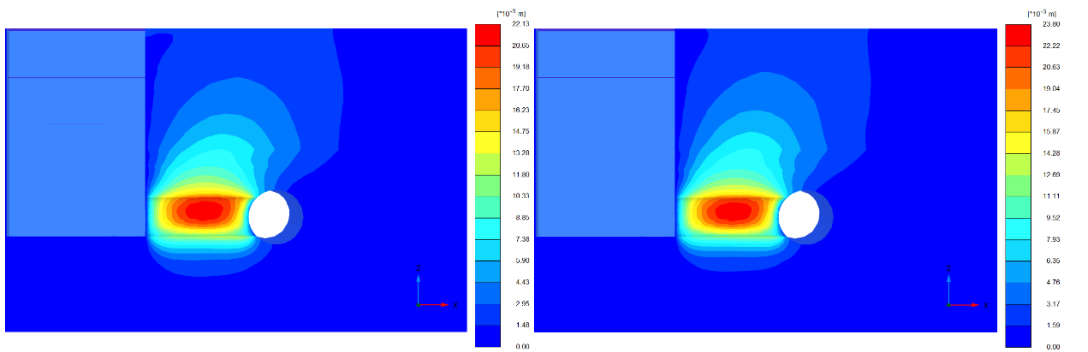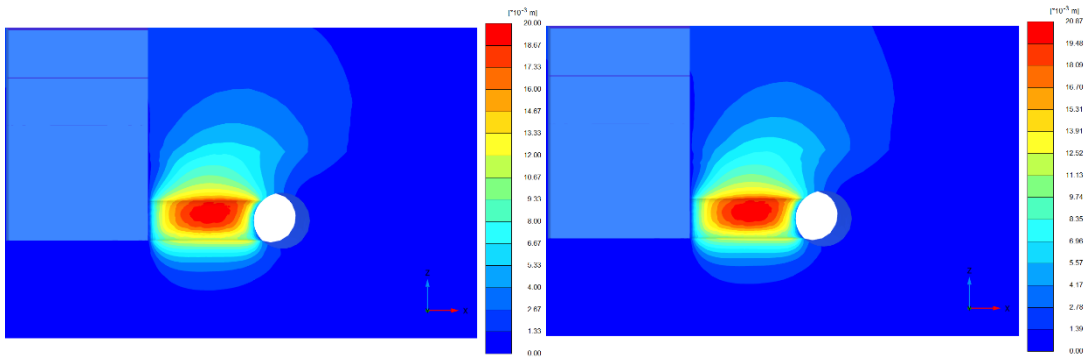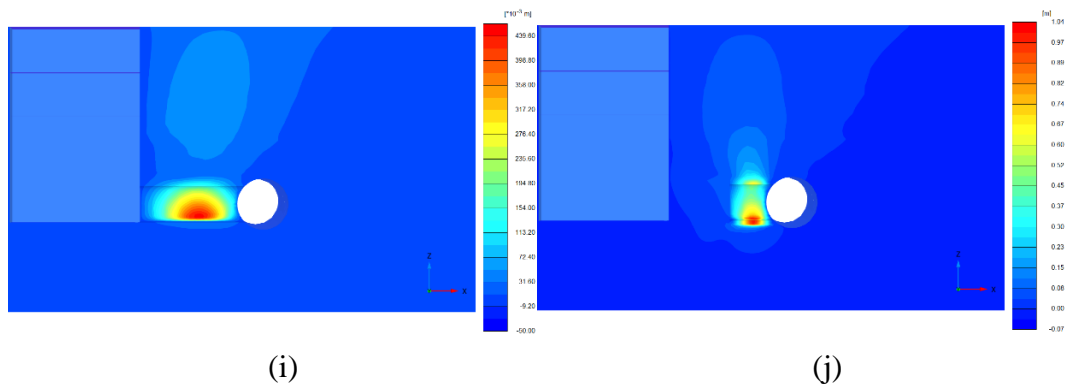
Figure 4-5. Total displacement of cross-passage at the final excavation stage in different ground improvement thickness schemes: (a) 3.0R; (b) 2.8R; (c) 2.6R; (d) 2.4R; (e) 2.2R; (f) 2.0R; (g) 1.8R; (h) 1.6R; (i) 1.4R; (j) 1.2R

Figure 4-4 and Figure 4-5 show the surface displacement and displacement of cross-passage in all directions of 10 different schemes. The maximum displacement occurred at the crown of the cross-passage (Figure 4-4). It is generally believed that the largest displacement takes place at the middle of the crown of the cross-passage in the tunnelling problem and decreases slightly when moving toward the ground surface. However, the ground surface settlement is not in the middle in this study due to the effects of the intervention shaft. Some lateral movement is also observed at the TBM tunnel side. As a result, the maximum ground surface displacement tends to occur near to the cross-passage face opening (Figure 4-5).
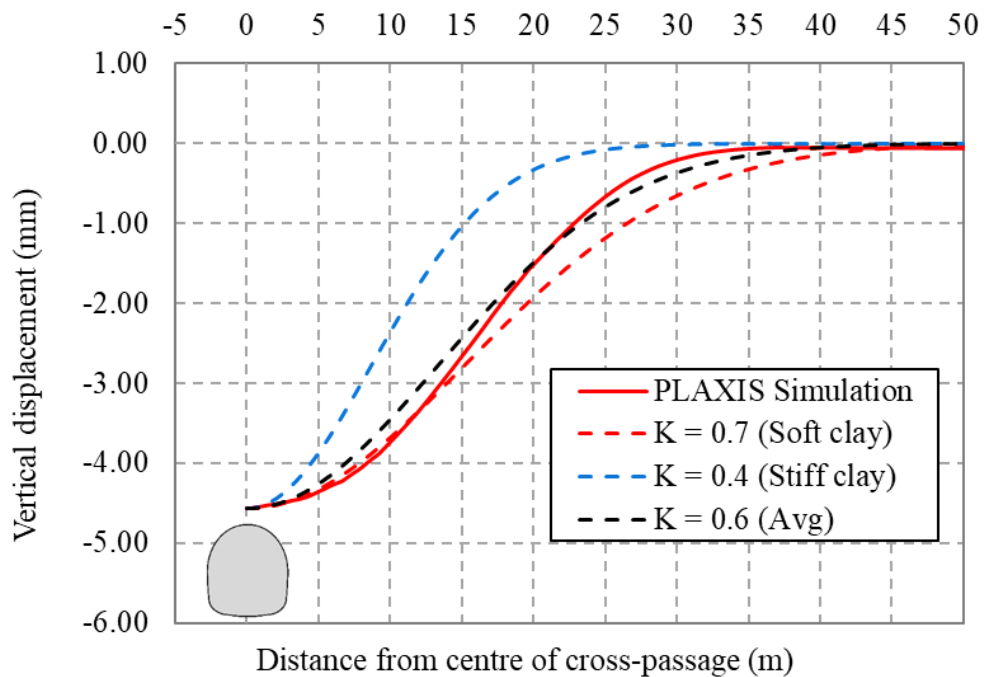
Figure 4-6. Ground surface profile induced by tunnel excavation of 1.6R scheme

As shown in Figure 4-6, the settlement profile from FEM fits well with the estimation by the empirical equation (2.8) and the settlement trough estimated according to O'Reilly and New (1982). The dash lines represent the predictions by empirical formula for various soil types. From the research of O'Reilly and New (1982), the K value varies from 0.4 (stiff clay) to 0.7 (soft clay) for the cohesive soil. Since the overburden layers in this study consist of stiff clay and soft clay, the average based on thickness of each soil type above the tunnel crown was used ($K = 0.6$). It can be seen that the shape of deformations of $K = 0.6$ fits well with the results from the FEA simulation. The green dash line ($K = 0.4$) significantly differs from the simulation result and the $K = 0.7$ line. It is the result of the overburden soil on the cross-passage mainly composes of soft clay which is up to 14m depth. However, the trend of the line for soft clay is quite similar although it is not fit well with the simulation result which is the effect of the stiff clay. Overall, the empirical coefficient $K = 0.6$ is the suitable value for this case and it also can be proved that the displacement from the 3D simulation is accurate.
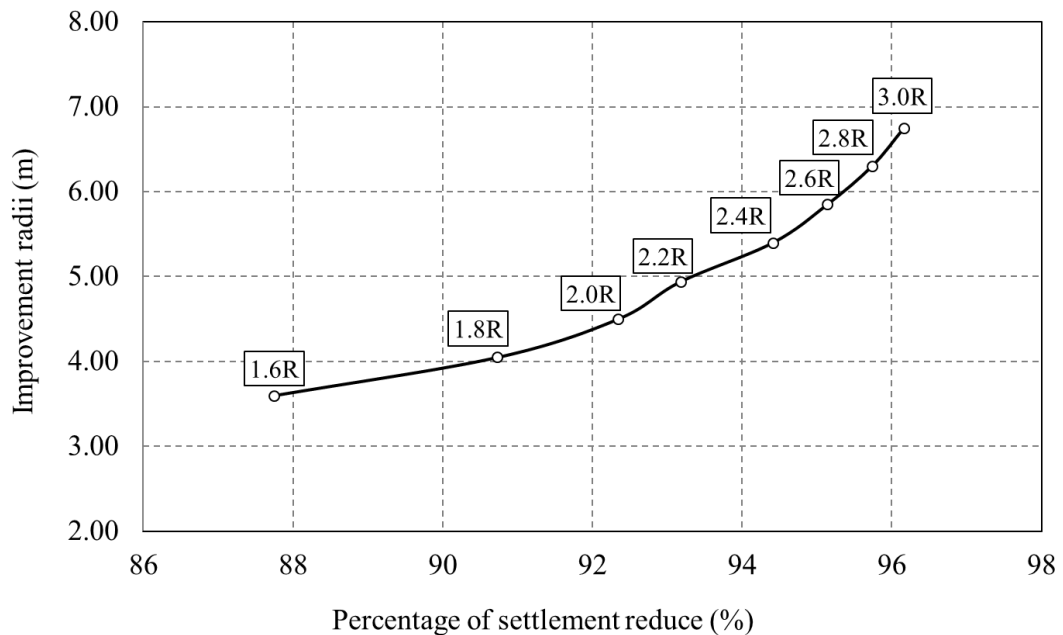
Figure 4-7. The percentage of settlement reduction in each scheme

Figure 4-7 shows the percentage of the settlement reduction from 1.6R to 3.0R improvement schemes. These values are compared to the maximum surface displacement of improvement scheme 1.2R which is 37.22mm. As a result of increasing the improvement radius, the percentage of settlement reduction increases significantly which start at the 1.6R improvement scheme about 87.75% and reach 96.20% at the 3.0R improvement scheme. For the 1.2R and 1.4R improvement schemes, the vertical displacement is so large and achieve instability.

4.3 Soil-cement Mixing Columns Arrangement

Recommendation of soil-cement columns arrangement of 1.6R scheme with the volume replacement ratio about 0.69 from equation (2.2). Figure 4-8 and Figure 4-9 show the layout of the soil-cement after arrangement in the plan view, cross-sectional view, and perspective view. The vertical thickness of soil-cement columns can be set easily while the horizontal thickness depends on the number of installation columns and the diameter of the soil-cement columns. In case the horizontal thickness does not reach the set value, other columns will be installed until it reaches the satisfied value. From the cross-sectional view, the soil improvement radius in vertical and oblique direction have the same value while the horizontal radius is larger.
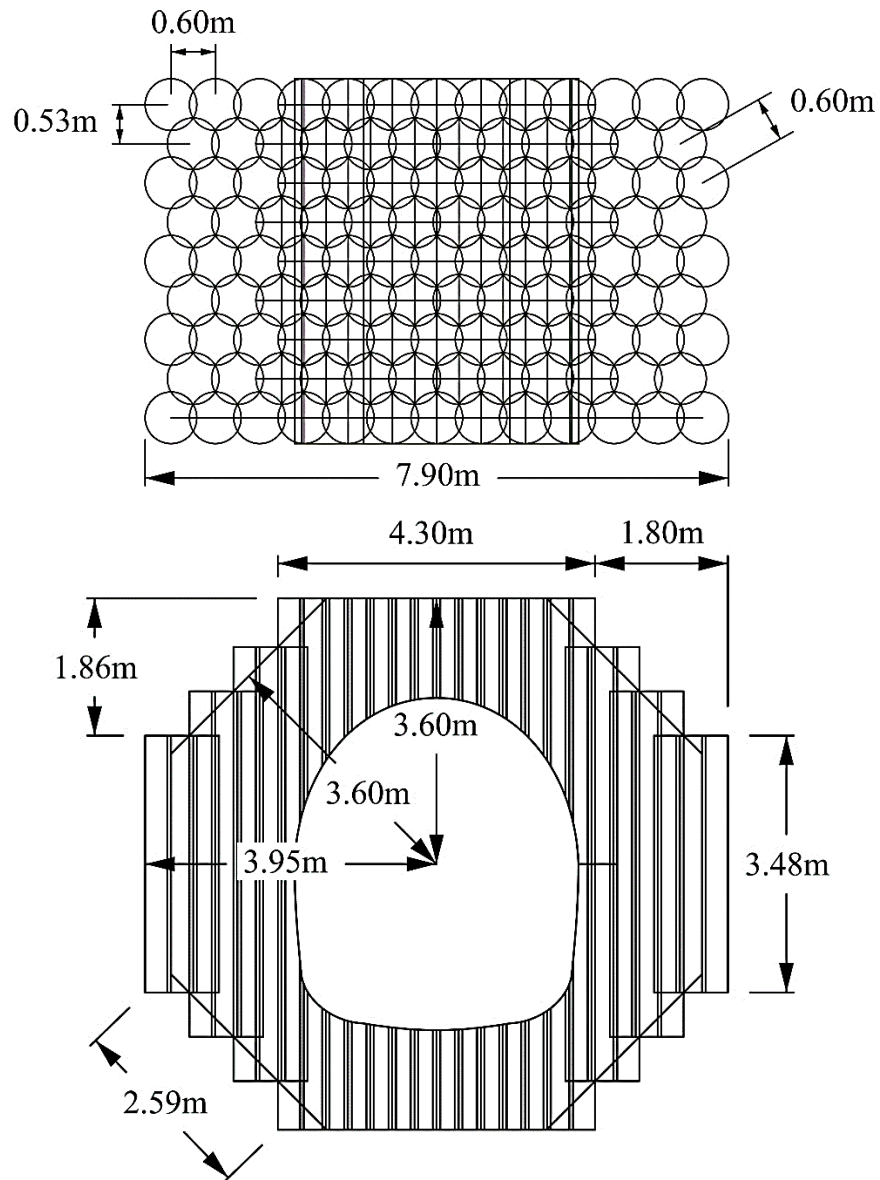
Figure 4-8. Plan view, and cross-sectional view of soil-cement columns after the arrangement.
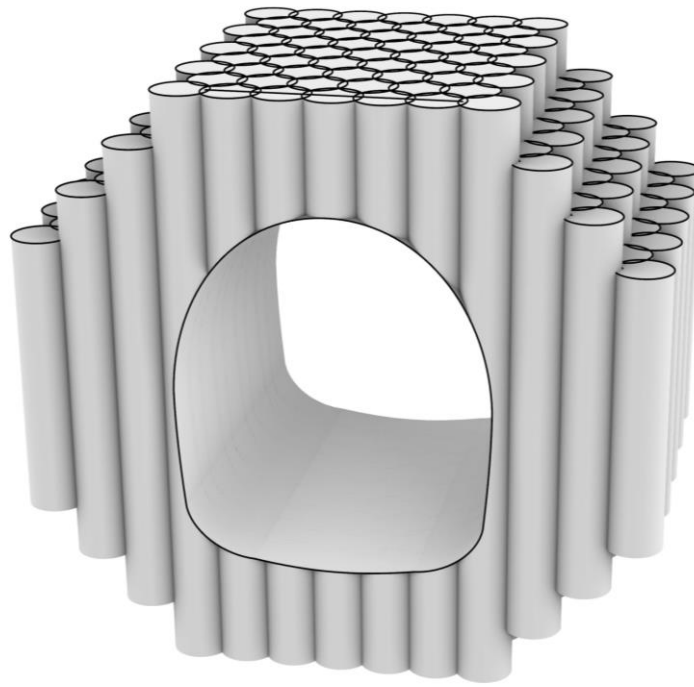
Figure 4-9. Perspective view of soil-cement columns after the arrangement.

CHAPTER 5

CONCLUSION AND RECOMMENDATIONS

5.1 Concluding Remark

Optimization based on the factor of safety indicated that the ground improvement 1.6R scheme (3.6m improvement radius) is the best choice for the reason that the safety factor is more than 1.40 and the thickness of the ground improvement is about 1.35m which is more than 0.1m required for preventing short term seepage problems.

The ground surface displacement of 1.6R improvement scheme is about 4.57mm. However, the ground surface settlement can be reduced by increasing the improvement radius (Figure 5-1). The settlement trough curve from the simulation is found to fit well with the empirical formula of O'Reilly when the empirical coefficient $K = 0.6$ is used.
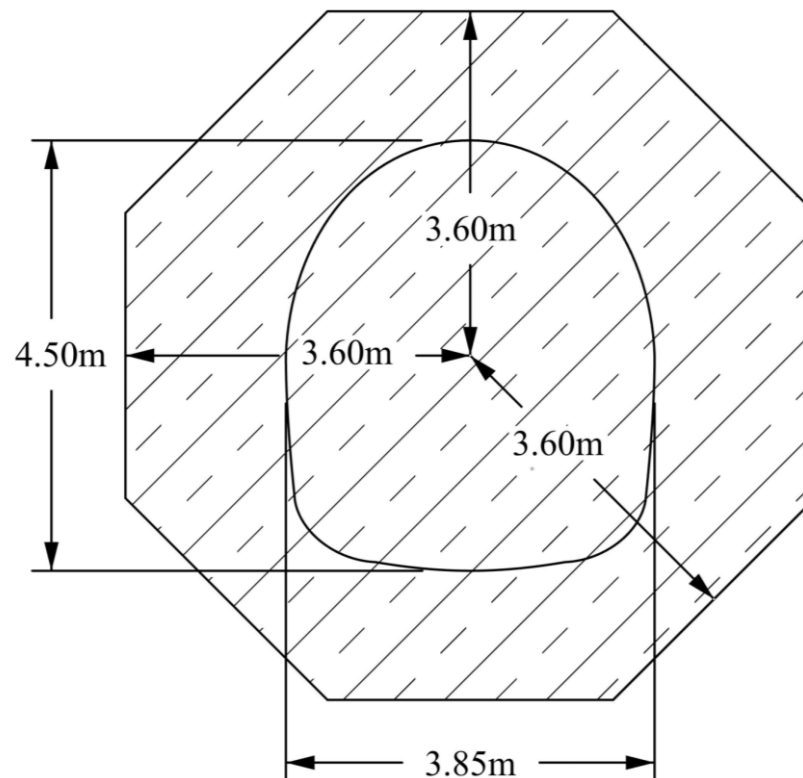
Figure 5-1. Soil mixing 1.6R scheme ($R_i = 3.60$m)

5.2 Work Summarizing

This study presents the three-dimensional finite element method to optimize the soil-cement on cross-passage based on the factor of safety and the thickness of the ground improvement. The ground was modelled by three soil layers systems which is referred to the borehole section A 23-AR 001 of the MRT blue line. The recovery drawdown pore water pressure is used which is refer to the data at the SBTA site. The thickness of soil-cement was varied from 1.2R to 3.0R. Hardening soil model (HSM) is used in this study. For FEA model is 80m wide by 50m long and 35m thick consisting of 84,484 nodes and 58,538 elements with average size elements of 1.785m. Hardening soil model is adopted for Bangkok subsoil while Mohr-coulomb soil model was used for soil-cement mixing. In each improvement scheme, 12 phases are used excluding the initial phase and the modelling time consuming is around 40 minutes for each scheme. Hence, the total time consuming is about 7 hours.

5.3 Recommendations and Future Research

- Validate with monitoring data should be conducted.
- Surrounding structures could be affected by excavation.
- Consolidation behaviour of soil should be considered.
- Effect from surcharge should be considered.

REFERENCES

A.Bruce, D. (2000). *An Introduction to the Deep Soil Mixing Methods as Used in Geotechnical Applications* (FHWA-RD-99-138). Retrieved from Turner-Fairbank Highway Research Center 6300 Georgetown Pike McLean, VA 22101:

Alipour, R., Khazaei, J., Pakbaz, M. S., & Ghalandarzadeh, A. (2017). Settlement control by deep and mass soil mixing in clayey soil. *Proceedings of the Institution of Civil Engineers - Geotechnical Engineering, 170*(1), 27-37. doi:10.1680/jgeen.16.00008

Andromalos, K. B., Hegazy, Y. A., & Jasperse, B. H. (2001). Stabilization of soft soils by soil mixing. In *Soft ground technology* (pp. 194-205).

Bickel, J. O., Kuesel, T. R., & King, E. H. (1996). *Tunnel Engineering Handbook* (2nd ed.). New York: Chapman & Hall.

Brinkgreve, R., Kumarswamy, S., Swolfs, W., Waterman, D., Chesaru, A., & Bonnier, P. (2016). PLAXIS 2016. *PLAXIS bv, the Netherlands*.

Broms, B. B., & Bennermark, H. (1967). Stability of clay at vertical openings. *Journal of Soil Mechanics & Foundations Div, 93*, 71 - 94.

Chai, J., & Carter, J. P. (2011). *Deformation Analysis in Soft Ground Improvement* (Vol. 18). New York: Springer Science & Business Media.

Chheng, C., & Likitlersuang, S. (2018). Underground excavation behaviour in Bangkok using three-dimensional finite element method. *Computers and Geotechnics, 95*, 68-81. doi:10.1016/j.compgeo.2017.09.016

Facibeni, L. (2019). Cross Passages : Design and Construction. In *Tunnel Design & Construction - Short Course*. Perth, Australia.

Fan, J., Wang, D., & Qian, D. (2018). Soil-cement mixture properties and design considerations for reinforced excavation. *Journal of Rock Mechanics and Geotechnical Engineering, 10*(4), 791-797. doi:10.1016/j.jrmge.2018.03.004

Filz, G. M., Adams, T., Navin, M. P., & Templeton, A. E. (2012). *Design of Deep Mixing for Support of Levees and Floodwalls*.

Gaur, A. (2017). Comparison of different soil models for excavation using retaining walls. *International Journal of Civil Engineering, 4*, 43-48. doi:10.14445/23488352/IJCE-V4I3P110

Han, J. (2015). *Principles and Practice of Ground Improvement*. Canada: John Wiley & Sons, Inc., Hoboken, New Jersey.

Horpibulsuk, S., Chinkulkijniwat, A., Cholphatsorn, A., Suebsuk, J., & Liu, M. D. (2012). Consolidation behavior of soil–cement column improved ground. *Computers and Geotechnics, 43*, 37-50. doi:10.1016/j.compgeo.2012.02.003

Horpibulsuk, S., Rachan, R., Suddeepong, A., & Chinkulkijniwat, A. (2011). Strength development in cement admixed Bangkok clay: laboratory and field investigations. *Soils and Foundations, 51*(2), 239-251.

Hwang, R., Ju, D. H., Tsai, M., & Fang, Y. (1995). Soft ground tunneling in Taiwan. *Proc., US/Taiwan Geotechnical Engineering*.

Jamsawang, P., Bergado, D. T., & Voottipruex, P. (2011). Field behaviour of stiffened deep cement mixing piles. *Proceedings of the Institution of Civil Engineers - Ground Improvement, 164*(1), 33-49. doi:10.1680/grim.900027

Jamsawang, P., Voottipruex, P., Boathong, P., Mairaing, W., & Horpibulsuk, S. (2015). Three-dimensional numerical investigation on lateral movement and factor of safety of slopes stabilized with deep cement mixing column rows. *Engineering Geology, 188*, 159-167. doi:10.1016/j.enggeo.2015.01.017

Jamsawang, P., Yoobanpot, N., Thanasisathit, N., Voottipruex, P., & Jongpradist, P. (2016). Three-dimensional numerical analysis of a DCM column-supported highway embankment. *Computers and Geotechnics, 72*, 42-56. doi:10.1016/j.compgeo.2015.11.006

Kitazume, M., & Terashi, M. (2013). *The deep mixing method*: CRC press.

Likitlersuang, S., Surarak, C., Suwansawat, S., Wanatowski, D., Oh, E., & Balasubramaniam, A. (2014). Simplified finite-element modelling for tunnelling-induced settlements. *Geotechnical Research, 1*(4), 133-152. doi:10.1680/gr.14.00016

Likitlersuang, S., Surarak, C., Wanatowski, D., Oh, E., & Balasubramaniam, A. (2013). Finite element analysis of a deep excavation: A case study from the Bangkok MRT. *Soils and Foundations, 53*(5), 756-773. doi:10.1016/j.sandf.2013.08.013

Lim, A., Ou, C.-Y., & Hsieh, P.-G. (2010). Evaluation of clay constitutive models for analysis of deep excavation under undrained conditions. *Journal of GeoEngineering, 5*(1), 9-20.

Lueprasert, P., Jongpradist, P., Charoenpak, K., Chaipanna, P., & Suwansawat, S. (2015). Three dimensional finite element analysis for preliminary establishment of tunnel influence zone subject to pile loading. *Maejo International Journal of Science and Technology, 9*, 209-223. doi:10.14456/mijst.2015.16

Meißner, H. (1996). Tunnelbau unter Tage. *Empfehlungen des Arbeitskreises l, 6*, 99.

Mihalis, I., Konstantis, S., Vlavianos, G., & Doulis, G. (2009). *Tunnel Stability Factor – A new controlling parameter for the face stability conditions of shallow tunnels in weak rock environment*. Paper presented at the International society for soil mechanics and geotechnical engineering, Egypt. https://www.issmge.org/uploads/publications/1/21/STAL9781607500315-2499.pdf

Möller, S. C. (2006). *Tunnel induced settlements and structural forces in linings.* (PhD Thesis). The University of Stuttgart, Institute of Geotechnical Engineering, Stuttgart, Germany, Retrieved from https://www.igs.uni-stuttgart.de/dokumente/Mitteilungen/54_Moeller.pdf

O'Reilly, M., & New, B. (1982). Settlements above tunnels in the United Kingdom-their magnitude and prediction. *Proceedings of the Third International Symposium, Tunnelling '82*(London, Institution of Mining and Metallurgy), 173-181.

Peck, R. B. (1969). Deep excavations and tunneling in soft ground. *Proceedings of the Seventh International Conference on Soil Mechanics and Foundation Engineering, Mexico, State of the Art Report*, 225 - 290.

Phienwaja, N. (1987). *Ground response and support performance in a sheared shale, Stillwater Tunnel, Utah.* (PhD). University of Illinois, Urbana-Champaign.

Saowiang, K., & Giao, P. H. (2020). Numerical analysis of subsurface deformation induced by groundwater level changes in the Bangkok aquifer system. *Acta Geotechnica*. doi:10.1007/s11440-020-01075-8

Schanz, T., Vermeer, P., & Bonnier, P. (1999). The hardening soil model: formulation and verification. *Beyond 2000 in computational geotechnics*, 281-296.

Schmidt, B. (1969). *Settlements and ground movements.* (Ph.D). Department of Civil Engineering, University of Illinois, Urbana, Illinois, 224 p.

Schweiger, H. (2009). *Influence of constitutive model and EC7 design approach in FEM analysis of deep excavations.* Paper presented at the Proceeding of ISSMGE International Seminar on Deep Excavations and Retaining Structures, Budapest.

Shibazaki, M. (2003). State of practice of jet grouting. In L. F. Johnsen, D. A. Bruce, & M. J. Byle (Eds.), *Grouting and Ground Treatment* (pp. 198-217). New Orleans, Louisiana, United States: American Society of Civil Engineers.

Sirivachiraporn, A., & Phienwej, N. (2012). Ground movements in EPB shield tunneling of Bangkok subway project and impacts on adjacent buildings. *Tunnelling and Underground Space Technology, 30*, 10-24. doi:10.1016/j.tust.2012.01.003

Surarak, C., Likitlersuang, S., Wanatowski, D., Balasubramaniam, A., Oh, E., & Guan, H. (2012). Stiffness and strength parameters for hardening soil model of soft and stiff Bangkok clays. *Soils and Foundations, 52*(4), 682-697. doi:10.1016/j.sandf.2012.07.009

Tan, Y. C., Koo, K. S., & Ting, D. I. (2019). Deep intervention shaft excavation in Kuala Lumpur limestone formation with pre-tunnelling construction method. In D. Peila, G. Viggiani, & T. Celestino (Eds.), *Tunnels and Underground Cities: Engineering and Innovation meet Archaeology, Architecture and Art – Peila, Viggiani & Celestino (Eds)* (pp. 1579-1588). Italy: CRC Press.

Tatiya, R. (2017). *Civil Excavations and Tunnelling: A practical guide* (H. Gulvanessian Ed. 2 ed.). Thomas Telford Ltd, 1 Heron Quay, London E14 4JD: ICE Publishing.

Topolnicki, M., & Pandrea, P. (2012). *Design of in-situ soil mixing.* Paper presented at the Proceedings of International Symposium on Ground Improvement, ISSMGE TC-211, Brussels, Belgium.

Usmani, A., Kannan, G., Nanda, A., & Jain, S. K. (2015). Seepage Behavior and Grouting Effects for Large Rock Caverns. *International Journal of Geomechanics, 15*(3). doi:10.1061/(asce)gm.1943-5622.0000449

Wang, D., Gao, Z., Lee, J. L., & Gao, W. (2014). Assessment and Optimization of Soil Mixing and Umbrella Vault Applied to a Cross-Passage Excavation in Soft Soils. *International Journal of Geomechanics, 14*(6). doi:10.1061/(asce)gm.1943-5622.0000374

Wijerathna, M., Liyanapathirana, S., & Leo, C. J. (2016). Consolidation behaviour of deep cement mixed column improved ground during breakage of soil-cement structure. *Australian Geomechanics Journal, 51*(2), 35 - 42.

Yee, Y. W., & Tan, Y. C. (2015). *Excavation support for TBM retrieval shaft using deep soil mixing technique, Kuala Lumpur*. Paper presented at the International Conference and Exhibition on Tunnelling and Underground Space.

APPENDICES

Appendix A
Summary Results of Cross-passage Stability

จุฬาลงกรณ์มหาวิทยาลัย
CHULALONGKORN UNIVERSITY
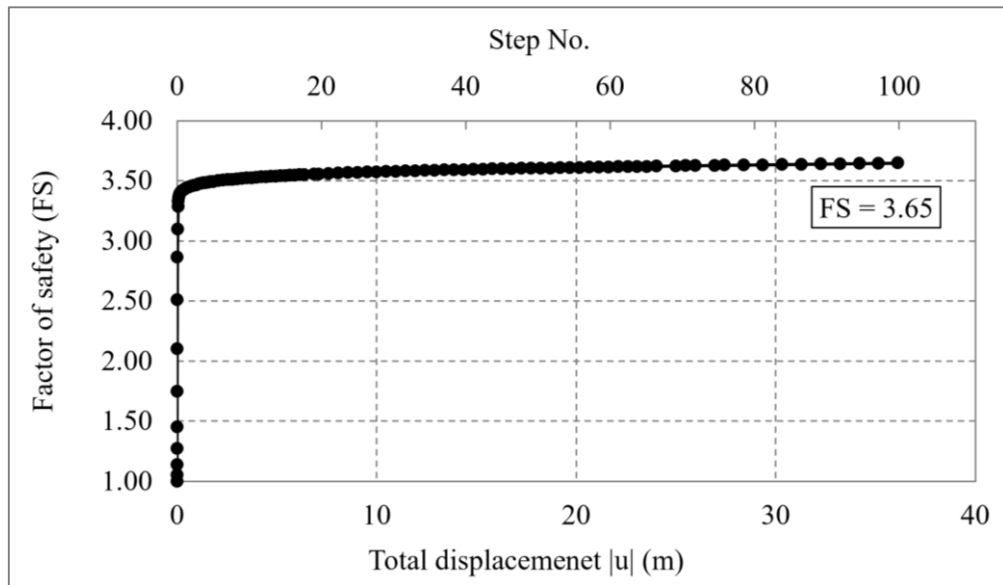
Figure A-1. Safety factor of 3.0R scheme
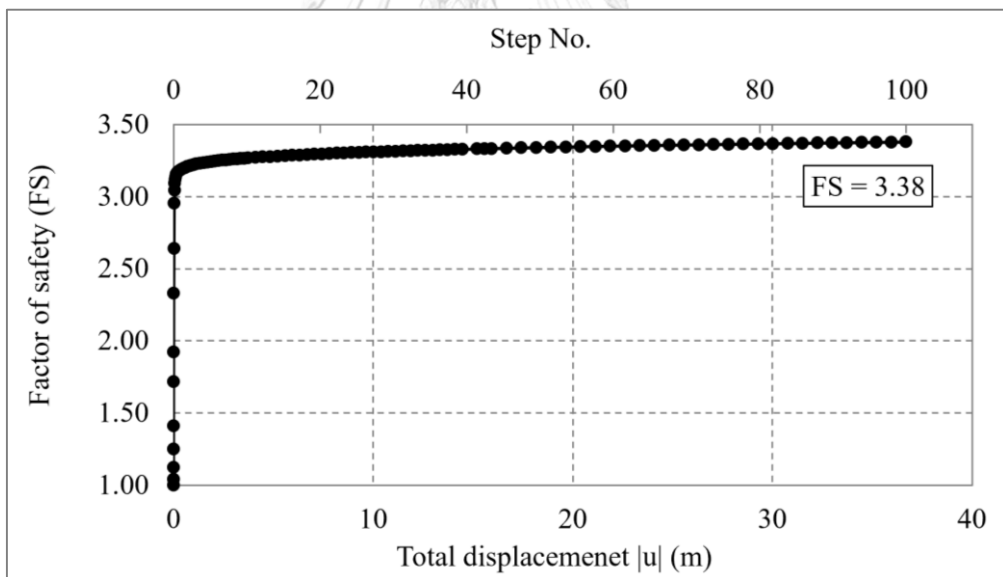
Figure A-2. Safety factor of 2.8R scheme
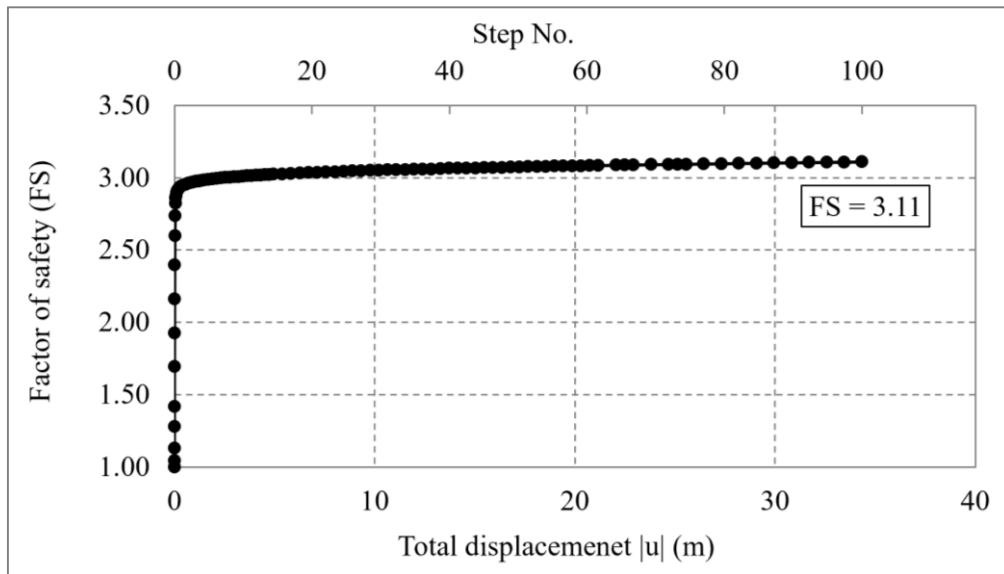
Figure A-3. Safety factor of 2.6R scheme
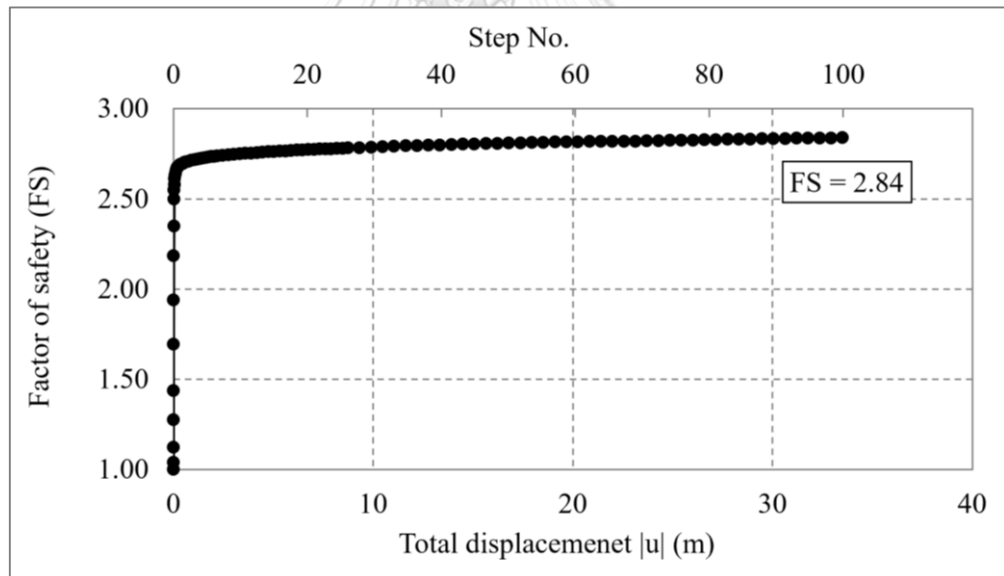
Figure A-4. Safety factor of 2.4R scheme
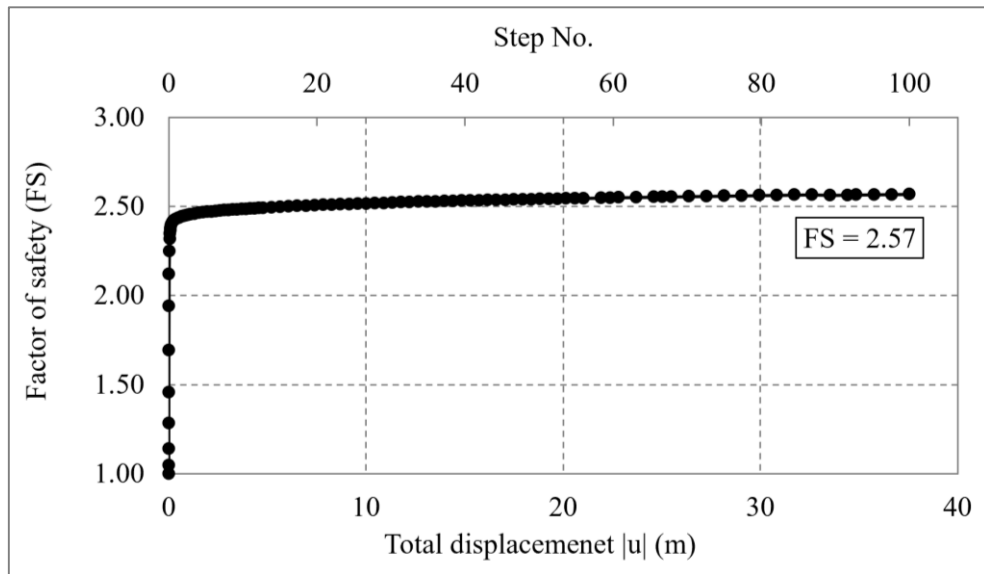
Figure A-5. Safety factor of 2.2R scheme
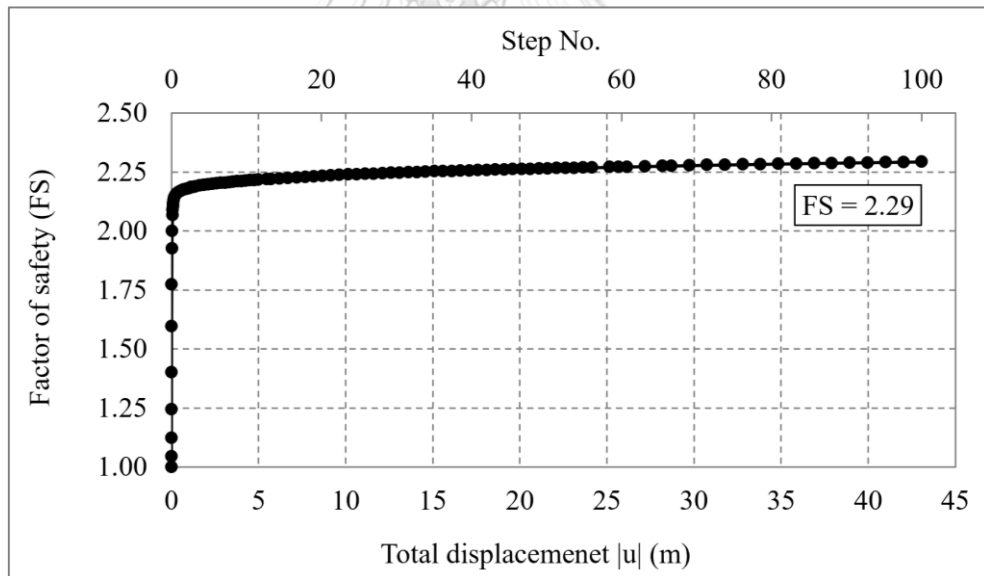
Figure A-6. Safety factor of 2.0R scheme
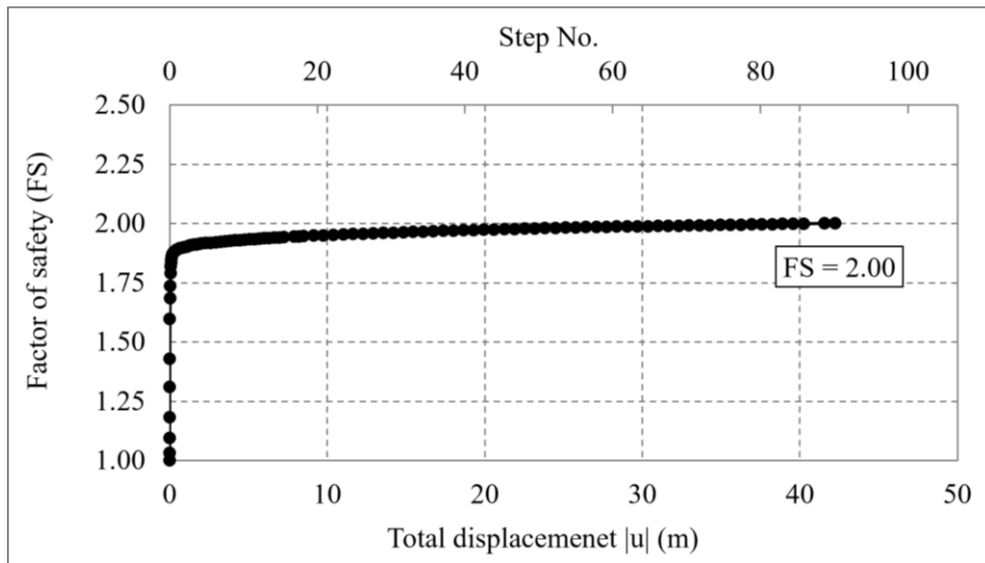
Figure A-7. Safety factor of 1.8R scheme
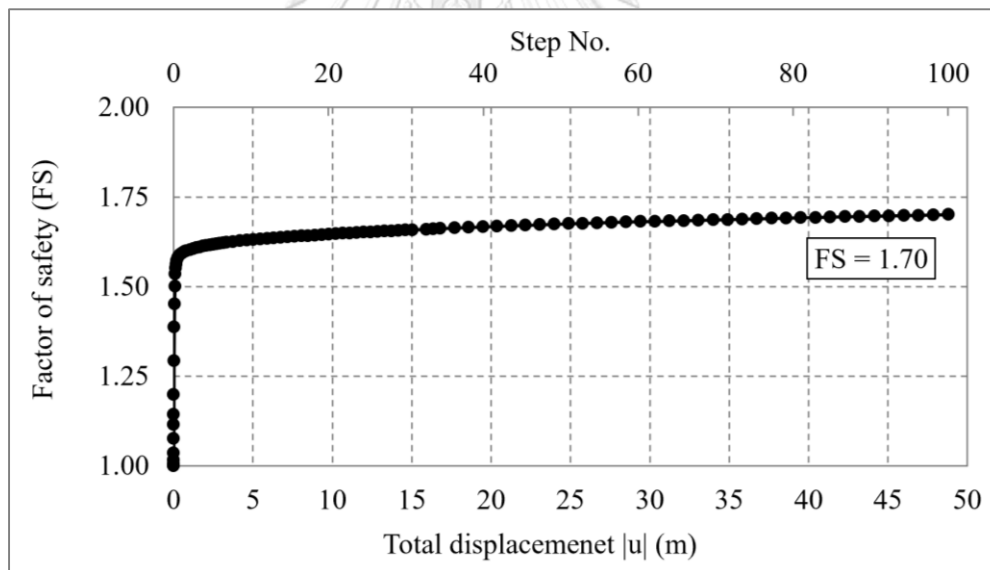
Figure A-8. Safety factor of 1.6R scheme
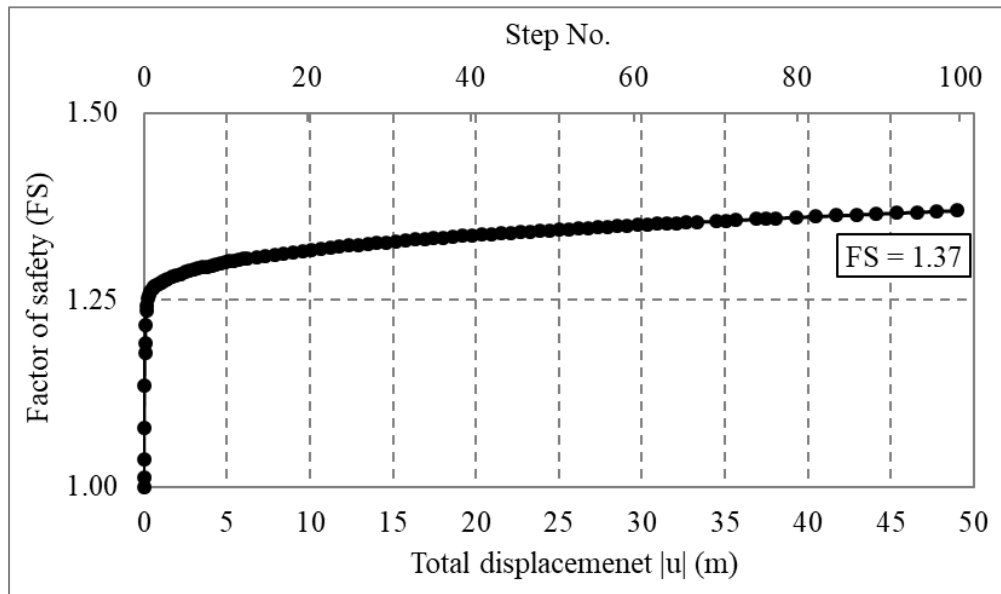
Figure A-9. Safety factor of 1.4R scheme
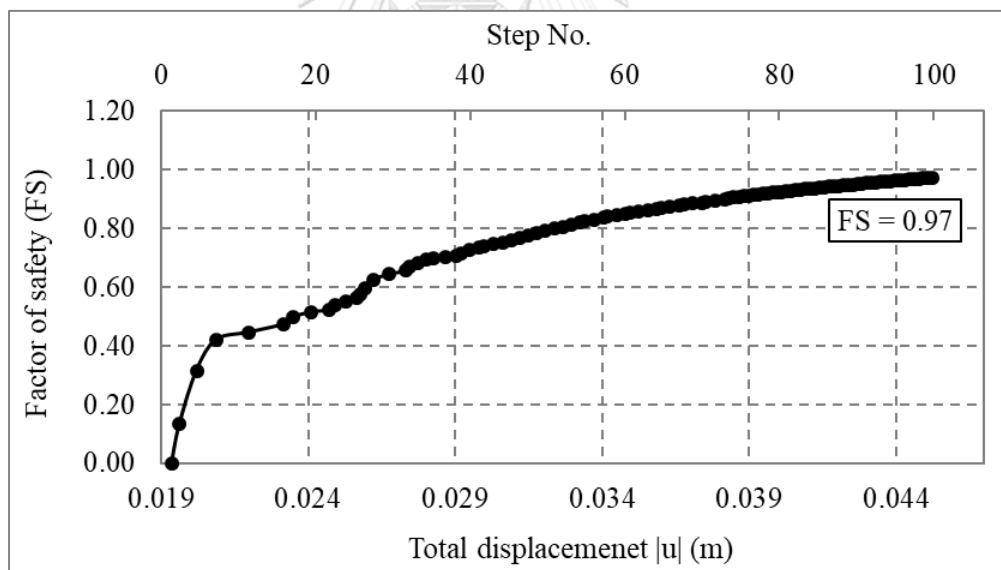
Figure A-10. Safety factor of 1.2R scheme

Appendix B
Ground Surface Displacement in each Scheme
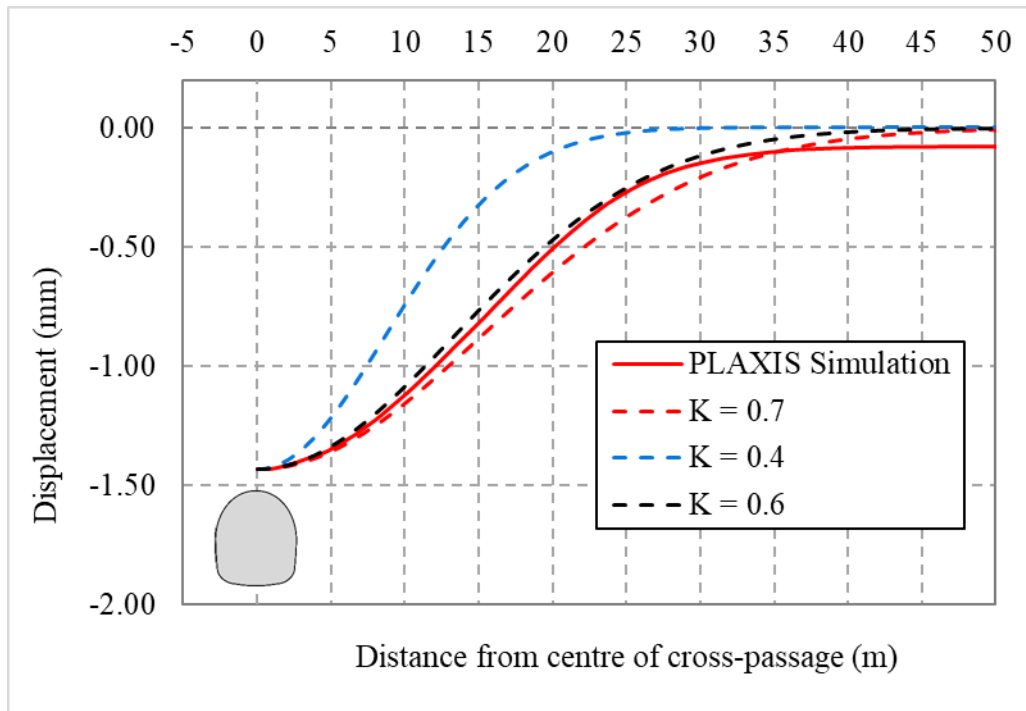
Figure B-1. Surface settlement trough of 3.0R scheme
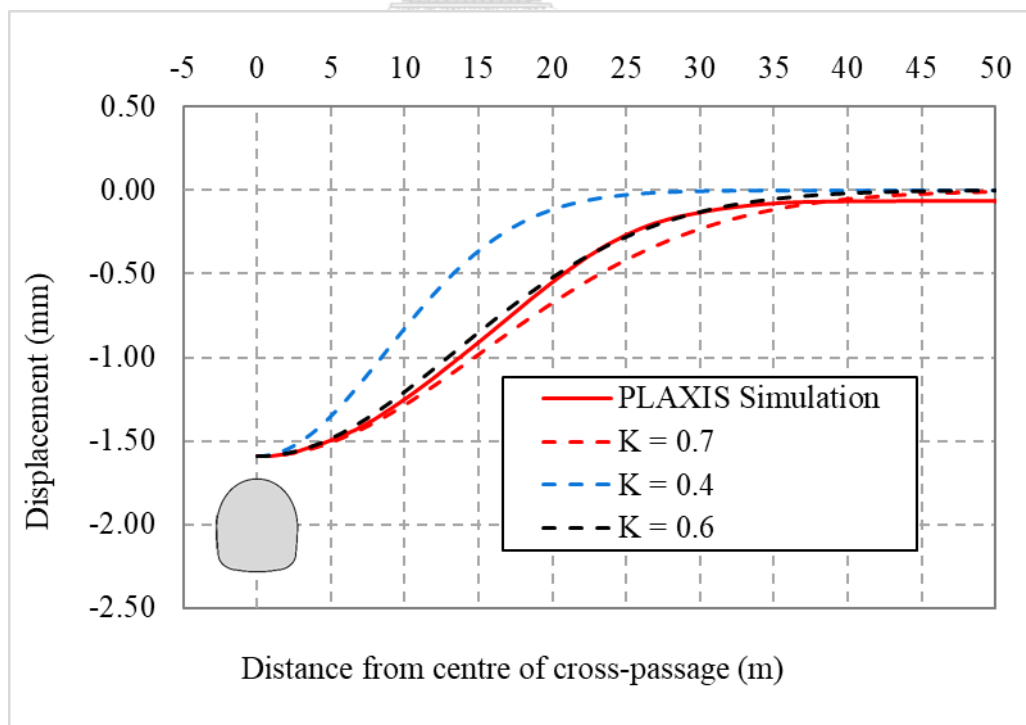
Figure B-2. Surface settlement trough of 2.8R scheme
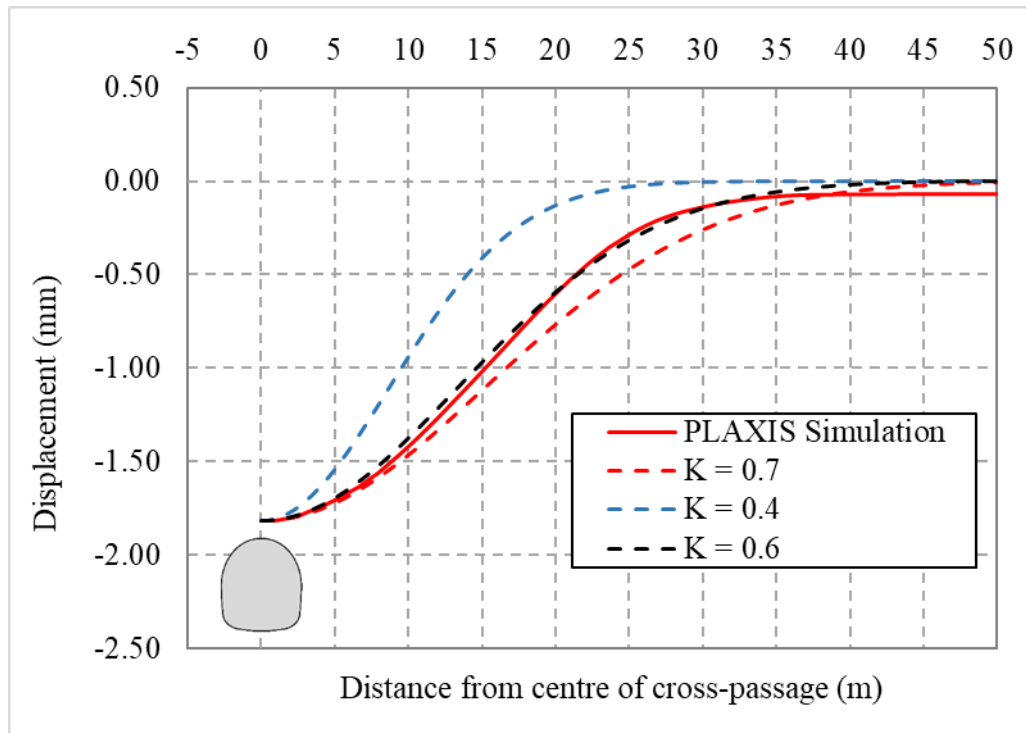
Figure B-3. Surface settlement trough of 2.6R scheme
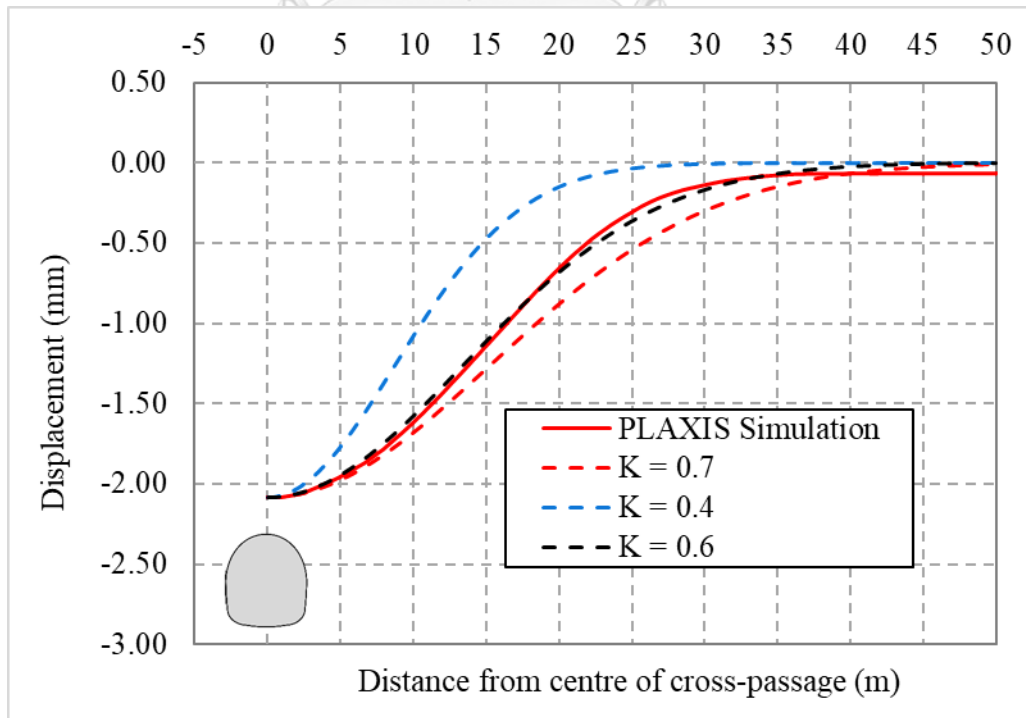
Figure B-4. Surface settlement trough of 2.4R scheme
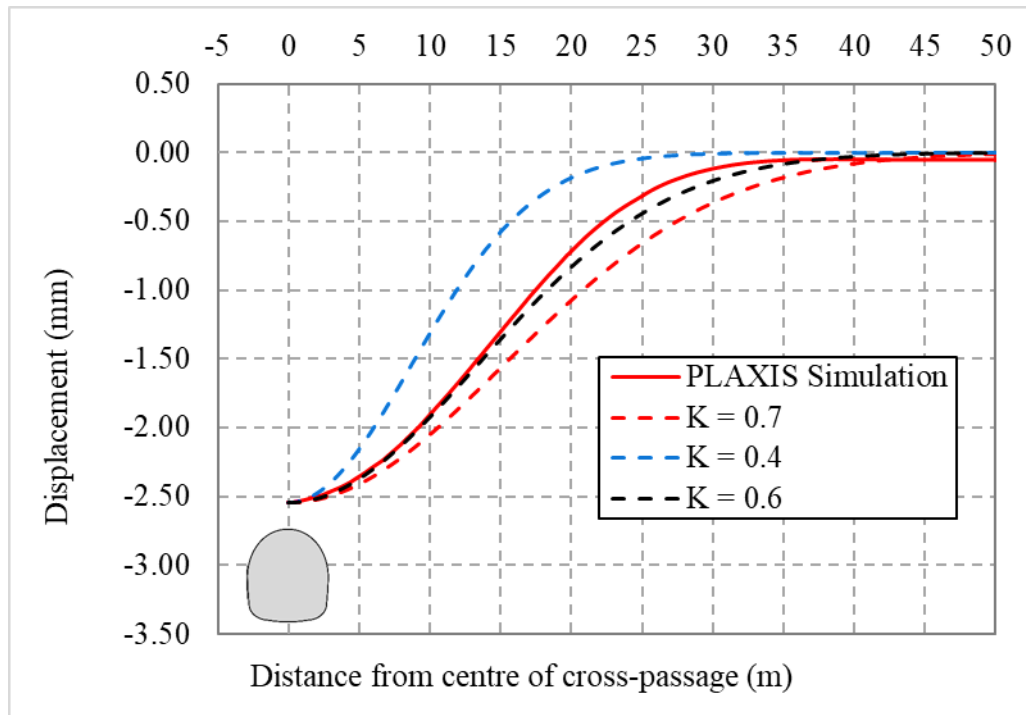
Figure B-5. Surface settlement trough of 2.2R scheme
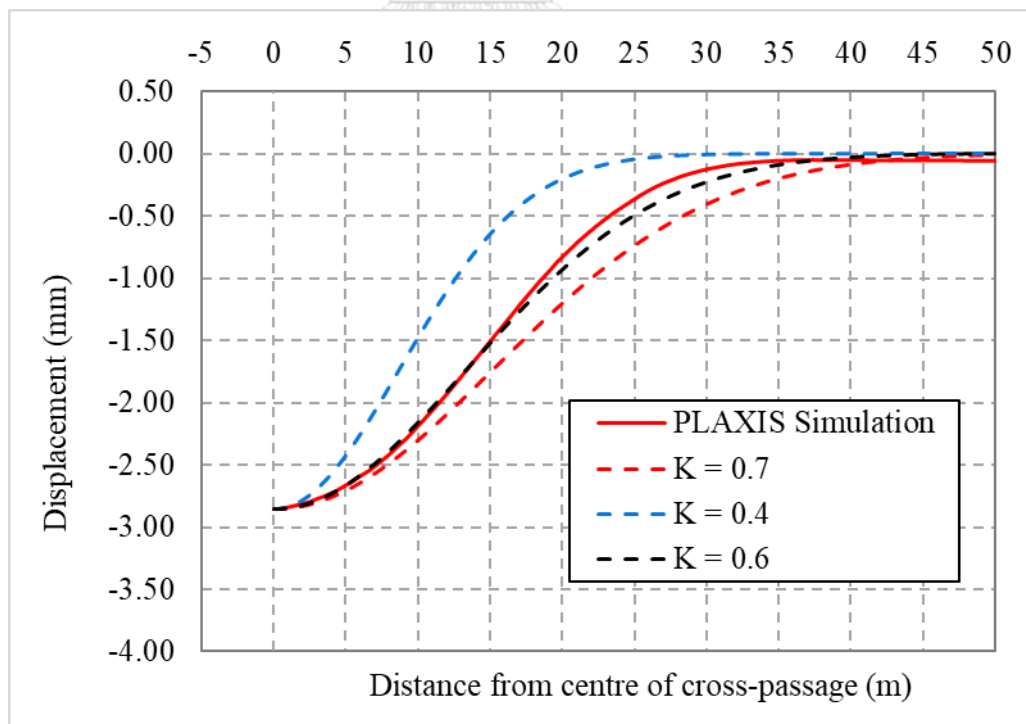
Figure B-6 Surface settlement trough of 2.0R scheme
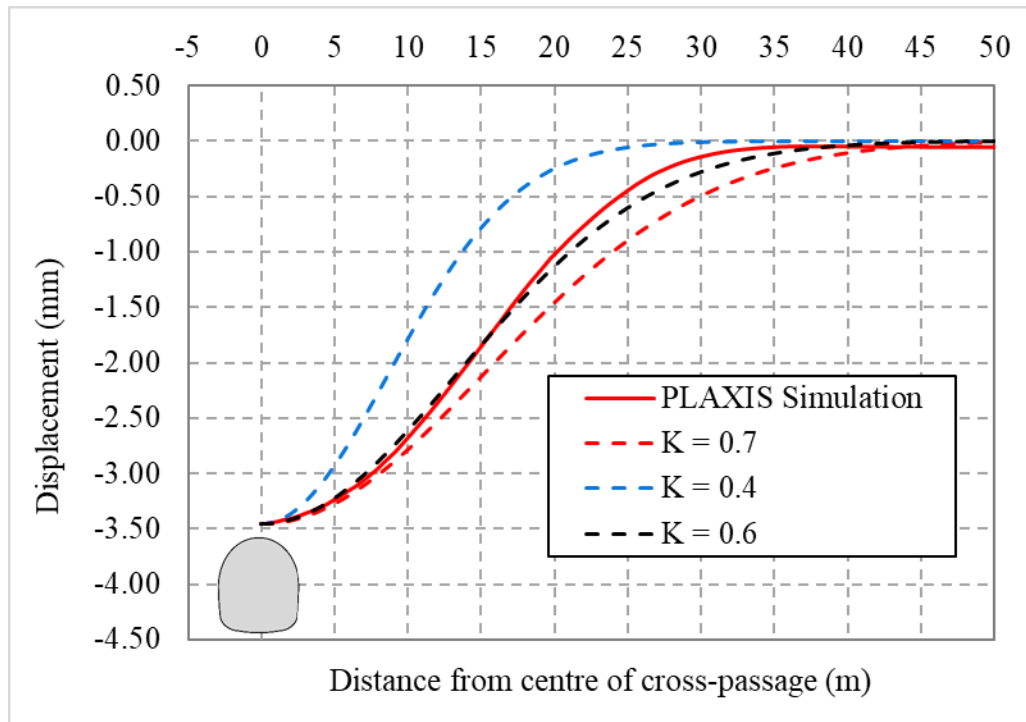
Figure B-7. Surface settlement trough of 1.8R scheme
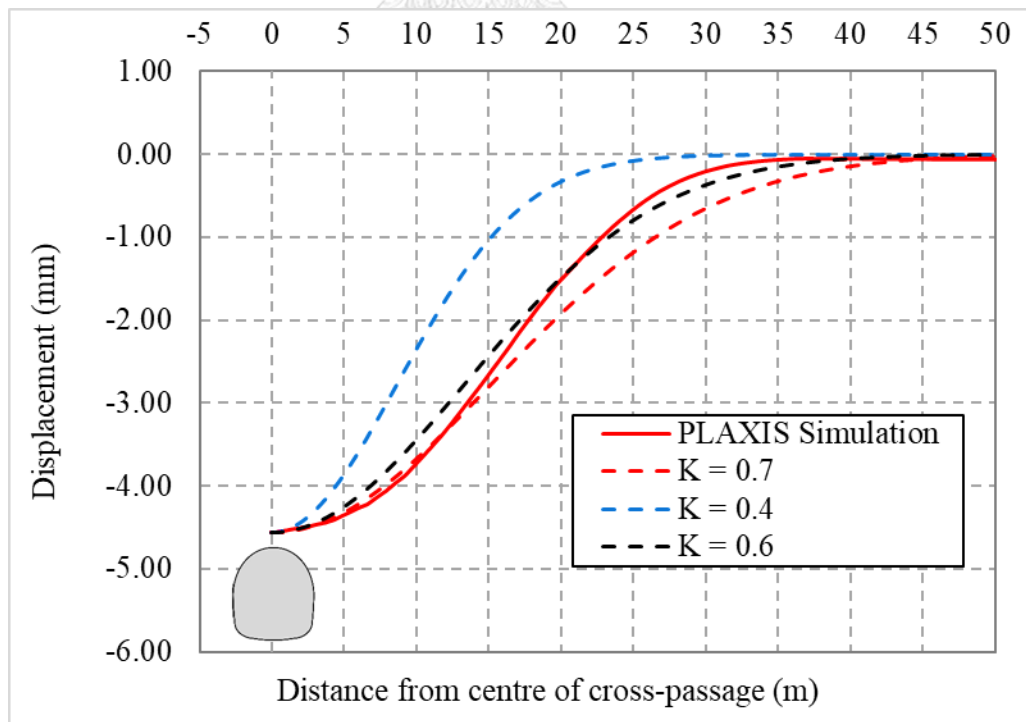
Figure B-8. Surface settlement trough of 1.6R scheme
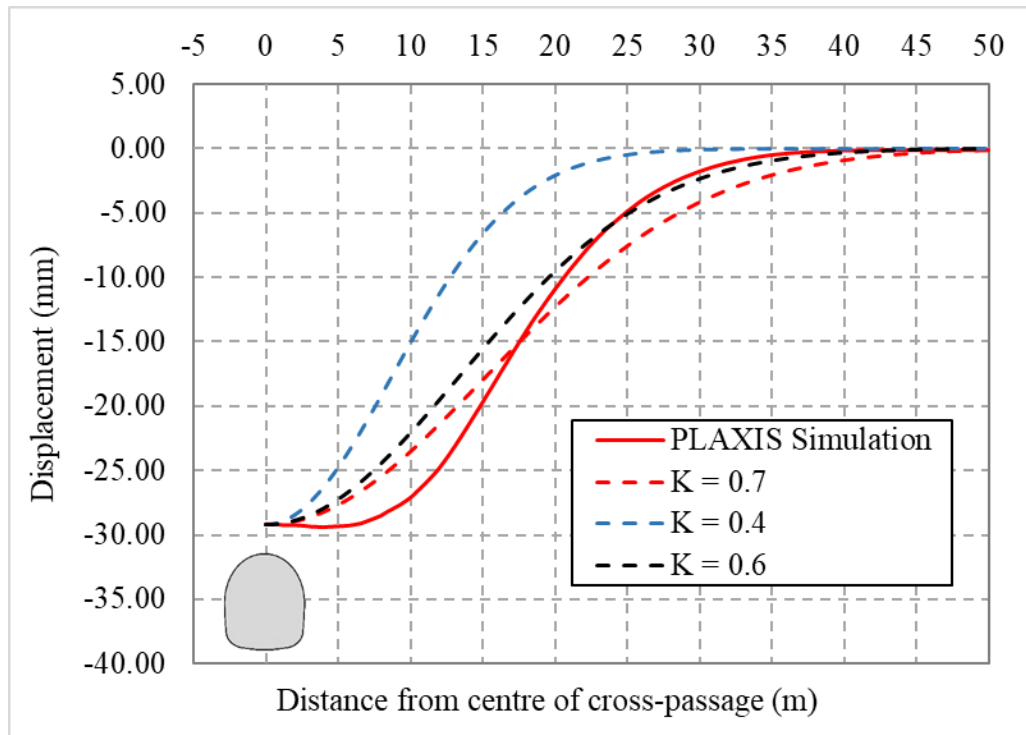
Figure B-9 Surface settlement trough of 1.4R scheme
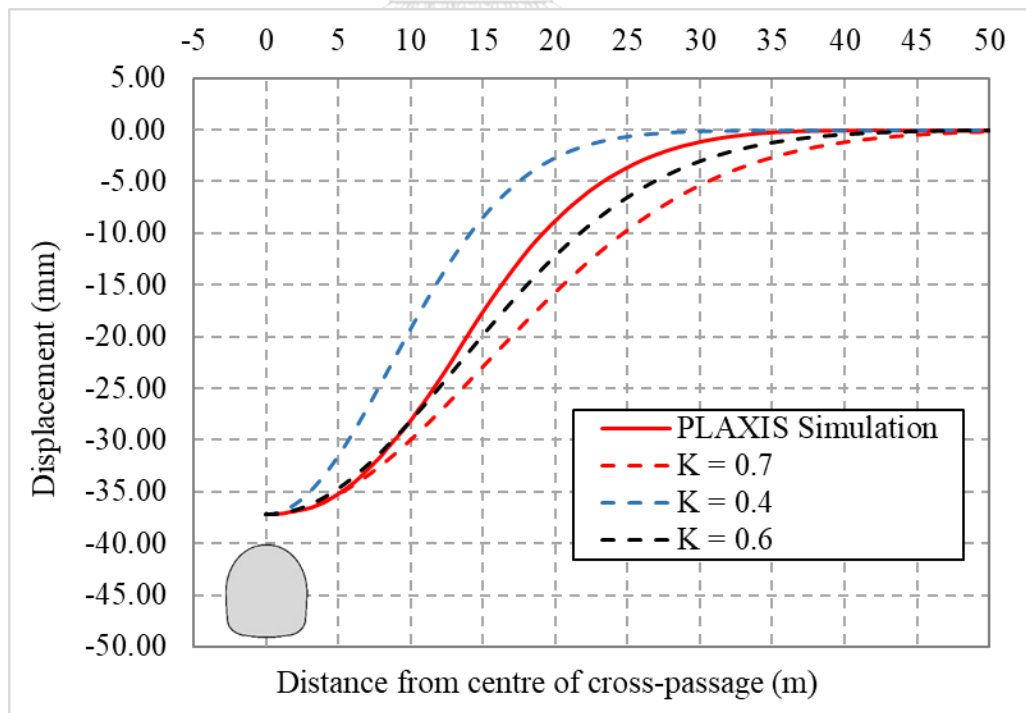
Figure B-10. Surface settlement trough of 1.2R scheme

VITA

NAME   Mengly Seng

DATE OF BIRTH   25 March 1995

PLACE OF BIRTH   Phnom Penh

INSTITUTIONS ATTENDED   Institute of Technology of Cambodia

HOME ADDRESS   No.25, St.234, Sangkat Phsar Deum Kor, Klan Toul Kork, Phnom Penh, Cambodia